

# Embedding Principle in Depth for the Loss Landscape Analysis of Deep Neural Networks

Zhiwei Bai<sup>1</sup>, Tao Luo<sup>1</sup>, Zhi-Qin John Xu<sup>1\*</sup>, Yaoyu Zhang<sup>1,2†</sup>

<sup>1</sup> School of Mathematical Sciences, Institute of Natural Sciences, MOE-LSC and Qing Yuan Research Institute, Shanghai Jiao Tong University

<sup>2</sup> Shanghai Center for Brain Science and Brain-Inspired Technology  
{bai299, luotao41, xuzhiqin, zhyy.sjtu}@sjtu.edu.cn.

## Abstract

Understanding the relation between deep and shallow neural networks is extremely important for the theoretical study of deep learning. In this work, we discover an embedding principle in depth that loss landscape of an NN “contains” all critical points of the loss landscapes for shallower NNs. The key tool for our discovery is the critical lifting operator proposed in this work that maps any critical point of a network to critical manifolds of any deeper network while preserving the outputs. This principle provides new insights to many widely observed behaviors of DNNs. Regarding the easy training of deep networks, we show that local minimum of an NN can be lifted to strict saddle points of a deeper NN. Regarding the acceleration effect of batch normalization, we demonstrate that batch normalization helps avoid the critical manifolds lifted from shallower NNs by suppressing layer linearization. We also prove that increasing training data shrinks the lifted critical manifolds, which can result in acceleration of training as demonstrated in experiments. Overall, our discovery of the embedding principle in depth uncovers the depth-wise hierarchical structure of deep learning loss landscape, which serves as a solid foundation for the further study about the role of depth for DNNs.

## 1 Introduction

It has been widely observed that overparameterized deep neural networks (DNNs) often generalize well in practice. This is a mystery that remains unsolved for decades in deep learning theory (Breiman 1995; Zhang et al. 2017). A highly relevant observation is that narrower or shallower NNs can often achieve similar accuracy as larger networks when smaller networks are trained to mimic the predictions of larger networks (Ba and Caruana 2014; Romero et al. 2015). Recently, the discovery of embedding principle provides insight to this phenomenon through loss landscape analysis (Zhang et al. 2021b, 2022; Fukumizu et al. 2019; Simsek et al. 2021). By the embedding principle, i.e., loss landscape of an NN “contains” all critical points of loss landscapes for narrower NNs, training of a wide NN can be attracted to “simple” critical points embedded from narrower NNs to avoid overfitting. Inspired by the discovery of embedding principle regarding DNNs of different widths

\*Corresponding author: xuzhiqin@sjtu.edu.cn.

†Corresponding author: zhyy.sjtu@sjtu.edu.cn.

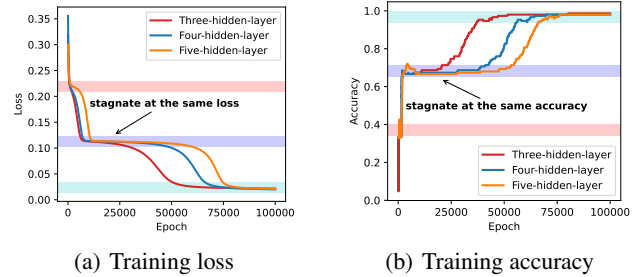


Figure 1: (a) The training loss for NNs of different depths on Iris dataset. The colored spans indicate where the training loss decays slowly, possibly experienced a saddle point. (b) The training accuracy for NNs of different depths on Iris dataset. The colored spans of accuracy in (b) correspond to the same colored spans of loss value in (a).

(referred to as the embedding principle in width in the following), we study in this work the relation between loss landscapes of shallow and deep networks due to the extreme importance of depth for DNNs. Specifically, we discover the embedding principle in depth detailed in the following, which firmly support the observed training and generalization similarity among DNNs of different depths.

Our theoretical study is motivated by the following experiment, observation of which provides evidence to the existence of an embedding relation in depth. In Fig. 1(a), training trajectories of NNs with 3, 4 and 5 hidden layers are shown to learn the Iris dataset (Fisher 1936). Surprisingly, their training trajectories stagnate at almost the same loss values with almost the same training accuracy as demonstrated in Fig. 1(b). This phenomenon suggests that loss landscapes of NNs of different depths share a set of critical functions (i.e., output functions of critical points), by which a deep NN can experience a training process similar to that of a shallower NN. Remark that, a similar phenomenon can be observed regarding the training of wide and narrow NNs (Zhang et al. 2021b).

Motivated by above observation, we prove in this work an embedding principle in depth for fully-connected NNs stated *intuitively* as follows:

**Embedding principle in depth:** *the loss landscape of any*

network “contains” all critical points of all shallower networks.

Key to our proof of embedding principle in depth is a critical lifting operator proposed in this work, which maps any critical point of a shallower NN to critical manifolds (i.e., manifolds consisting of critical points with the same loss value) of a target NN preserving outputs on the training inputs. Our critical lifting operator predicts a rich class of “simple” critical points from shallower NNs in the loss landscapes of deep NNs. Our numerical study demonstrates that these lifted critical points indeed can be experienced during the practical training of deep NNs. We also demonstrate that, through critical lifting, local minima or non-strict saddle points transition to strict saddle points of deeper NNs, which can be easily escaped using first-order optimization methods (Lee et al. 2019). The embedding principle in depth also provides new understanding to the optimization benefits of batch normalization (Ioffe and Szegedy 2015) and large dataset, and highlights a layer pruning method as demonstrated by numerical experiments in Section 5.

The contribution of our work is summarized as follows:

- (i) We discover a general embedding principle in depth, which shows that loss landscape of a deep NN inherits all critical points from shallower NNs.
- (ii) We propose a critical lifting operator, which explicitly characterizes the hierarchy of critical manifolds from shallower NNs in an NN loss landscape.
- (iii) The critical lifting unravels a general strategy to avoid lifted critical manifolds through suppressing layer linearization, which provides new insight to batch normalization and large dataset.
- (iv) The critical lifting highlights a layer pruning approach of detecting and merging effectively linear layers.

Remark that, all proofs for our theoretical results and code for experiments are provided in Supplements.

## 2 Related Works

The loss landscape of DNNs is often very complex in general (Skorokhodov and Burtsev 2019). Different directions of a minimum can have very different sharpness (He, Huang, and Yuan 2019). Moreover, different training algorithms find global minima with different properties, such as SGD often finds a flatter minimum compared with GD (Keskar et al. 2017; Wu, Zhu et al. 2017). The loss landscape of shallow NNs with specific activations has also been studied in detail (Du and Lee 2018; Soltanolkotabi, Javanmard, and Lee 2018; Cheridito, Jentzen, and Rossmannek 2021). However, these works do not discuss the relation of critical points among different network structures.

Recently, Zhang et al. (2021b) proves an embedding principle by proposing one-step embeddings and their multi-step composition. It shows that the critical points of the loss landscape of a network can be embedded to critical points of the loss landscape for wider NNs. Similar results on these composition embeddings are studied for shallow NNs (Fukumizu and Amari 2000) and deep NNs (Fukumizu et al. 2019; Simsek et al. 2021). Zhang et al. (2022) further proposes a

wider family of general compatible embeddings to study the embedding principle in width. Different from these works studying the effect of width, our work for the first time establishes the embedding relation regarding the extremely important hyperparameter of depth for DNNs.

Using a deeper NN has many advantages. In approximation, a deeper NN has more expressive power (Telgarsky 2016; Eldan and Shamir 2016; E and Qingcan 2018). In optimization, a deeper NN can learn data faster (He et al. 2016; Arora, Cohen, and Hazan 2018; Xu and Zhou 2021). In generalization, a deeper NN may achieve better generalization for real-world problems (He et al. 2016). Therefore, it is important to understand the effect of depth to the DNN loss landscapes.

The embedding principle in depth implies a simplicity bias in depth, which is consistent with previous works, for example, the frequency principle (Xu, Zhang, and Xiao 2019; Xu et al. 2020; Rahaman et al. 2019; Zhang et al. 2021a), which states that DNNs often fit target functions from low to high frequencies during the training.

## 3 Preliminaries

### 3.1 Deep Neural Networks

Consider a fully-connected NN with  $L(L \geq 1)$  layers. For any  $i, k \in \mathbb{N}$  and  $i < k$ , we denote  $[i : k] = \{i, i+1, \dots, k\}$ . In particular, we denote  $[k] := \{1, 2, \dots, k\}$ . We regard the input as layer 0 and the output as layer  $L$ . The width of layer  $l$  is denoted as  $m_l$  and  $m_0 = d, m_L = d'$ . For any parameter  $\theta$  of the NN, we regard it as a  $2L$ -tuple  $\theta = (\theta_{|1}, \dots, \theta_{|L}) = (\mathbf{W}^{[1]}, \mathbf{b}^{[1]}, \dots, \mathbf{W}^{[L]}, \mathbf{b}^{[L]})$ , where  $\mathbf{W}^{[l]} \in \mathbb{R}^{m_l \times m_{l-1}}$  and  $\mathbf{b}^{[l]} \in \mathbb{R}^{m_l}$  are the weight and bias, respectively. The  $l$ -th layer parameters of  $\theta$  is the ordered pair  $\theta_{|l} = (\mathbf{W}^{[l]}, \mathbf{b}^{[l]})$ ,  $l \in [L]$ .

Given parameter vector  $\theta$ , we can define the neural network function  $\mathbf{f}_\theta(\cdot)$  recursively. First, we write  $\mathbf{f}_\theta^{[0]}(\mathbf{x}) = \mathbf{x}$  for all  $\mathbf{x} \in \mathbb{R}^d$ . Then for  $l \in [L-1]$ ,  $\mathbf{f}_\theta^{[l]}$  is defined recursively as  $\mathbf{f}_\theta^{[l]}(\mathbf{x}) = \sigma(\mathbf{W}^{[l]} \mathbf{f}_\theta^{[l-1]}(\mathbf{x}) + \mathbf{b}^{[l]})$ . Finally, we denote  $\mathbf{f}_\theta(\mathbf{x}) = \mathbf{f}(\mathbf{x}, \theta) = \mathbf{f}_\theta^{[L]}(\mathbf{x}) = \mathbf{W}^{[L]} \mathbf{f}_\theta^{[L-1]}(\mathbf{x}) + \mathbf{b}^{[L]}$ .

**Definition 1 (deeper/shallower).** Given two NNs,  $\text{NN}(\{m_l\}_{l=0}^L)$  and  $\text{NN}'(\{m'_l\}, l \in \{0, 1, 2, \dots, q, \hat{q}, q+1, \dots, L\})$ . If  $m'_1 = m_1, \dots, m'_q = m_q, m'_{\hat{q}} \geq \min\{m_q, m_{q+1}\}, m'_{q+1} = m_{q+1}, \dots, m'_L = m_L$ , then we say  $\text{NN}'$  is one-layer deeper than  $\text{NN}$ , and  $\text{NN}$  is one-layer shallower than  $\text{NN}'$ .  $J$ -layer deeper (or shallower) is defined by the composition of one-layer deeper (or shallower).

An NN is deeper than another NN means that it can be obtained by inserting some layers with sufficient widths to another NN. Remark that, for the convenience of notation, layer index  $l$  for the deeper NN is used as a dummy index possessing a specific order  $\{0, 1, 2, \dots, q, \hat{q}, q+1, \dots, L\}$ .

### 3.2 Loss Function

Let  $S = \{(\mathbf{x}_i, \mathbf{y}_i)\}_{i=1}^n$  and  $S_x = \{\mathbf{x}_i\}_{i=1}^n$  denote the training data and training inputs, respectively, where  $\mathbf{x}_i \in \mathbb{R}^d$ ,

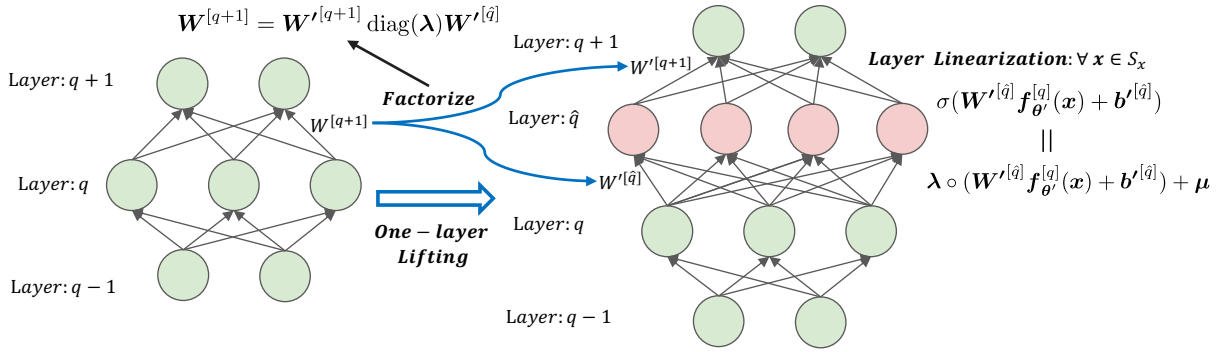


Figure 2: Illustration of one-layer lifting. The pink layer is inserted into the left network to get the right network. The input parameters  $\mathbf{W}'^{[\hat{q}]}$  and output parameters  $\mathbf{W}'^{[q+1]}$  of the inserted layer are obtained by factorizing the input parameters  $\mathbf{W}^{[q+1]}$  of  $(q+1)$ -th layer in the left network to satisfy layer linearization and output preserving conditions.

$\mathbf{y}_i \in \mathbb{R}^{d'}$ . For convenience, here we assume an unknown function  $\mathbf{f}^*$  satisfying  $\mathbf{f}^*(\mathbf{x}_i) = \mathbf{y}_i$  for  $i \in [n]$ . The empirical risk reads as  $R_S(\boldsymbol{\theta}) = \frac{1}{n} \sum_{i=1}^n \ell(\mathbf{f}(\mathbf{x}_i, \boldsymbol{\theta}), \mathbf{f}^*(\mathbf{x}_i)) = \mathbb{E}_S \ell(\mathbf{f}(\mathbf{x}, \boldsymbol{\theta}), \mathbf{f}^*(\mathbf{x}))$ , where the expectation  $\mathbb{E}_S h(\mathbf{x}) := \frac{1}{n} \sum_{i=1}^n h(\mathbf{x}_i)$  is defined for any function  $h: \mathbb{R}^d \rightarrow \mathbb{R}$ .

#### 4 Theory: Embedding Principle in Depth

Consider a neural network  $\mathbf{f}_{\boldsymbol{\theta}}(\mathbf{x})$ , where  $\boldsymbol{\theta}$  is the set of all network parameters,  $\mathbf{x} \in \mathbb{R}^d$  is the input. We summarize the assumptions for all our theoretical results in this work below.

**Assumption 1.** (i)  $L$ -layer ( $L \geq 1$ ) fully-connected NN.

(ii) Training data  $S = \{(\mathbf{x}_i, \mathbf{y}_i)\}_{i=1}^n$  for  $n \in \mathbb{Z}^+$ .

(iii) Empirical risk  $R_S(\boldsymbol{\theta}) = \mathbb{E}_S \ell(\mathbf{f}_{\boldsymbol{\theta}}(\mathbf{x}), \mathbf{y})$ .

(iv) Activation function  $\sigma$  has a non-constant linear segment, e.g., ReLU, leaky-ReLU and ELU.

(v) Loss function  $\ell$  and activation function  $\sigma$  are sub-differentiable, i.e., a unique subgradient can be assigned to each non-differentiable point.

**Remark.** For general smooth activations without a linear segment, e.g. tanh, our results hold in the sense of approximation because they are arbitrarily close to linear in a sufficiently small interval (say around 0). Therefore, we also demonstrate our results using the tanh activation in the following numerical experiments.

**Definition 2 (affine subdomain).** For activation  $\sigma$  with a non-constant linear segment, an affine subdomain of  $\sigma$  is an open interval  $(a, b)$  satisfying that there exist  $\lambda, \mu \in \mathbb{R}$  ( $\lambda \neq 0$ ),  $\sigma(x) = \lambda x + \mu$ , for any  $x \in (a, b)$ .

#### 4.1 Lifting Operator

We start from proposing a lifting operator as follows (see Fig. 2 for illustration).

**Definition 3 (one-layer lifting).** Given training data  $S$ , an NN  $(\{m_l\}_{l=0}^L)$  and a one-layer deeper NN'  $(\{m'_l\}, l \in \{0, 1, 2, \dots, q, \hat{q}, q+1, \dots, L\})$ , suppose  $m'_1 = m_1, \dots, m'_q = m_q, m'_{q+1} = m_{q+1}, \dots, m'_L = m_L$ . The one-layer lifting  $\mathcal{T}_S$  maps any parameter  $\boldsymbol{\theta} = (\mathbf{W}^{[1]}, \mathbf{b}^{[1]}, \dots, \mathbf{W}^{[L]}, \mathbf{b}^{[L]})$  of NN to a manifold  $\mathcal{M}(\mathcal{M} := \mathcal{T}_S(\boldsymbol{\theta}))$  of NN's parameter space, where

$\mathcal{M}$  is a collection of all  $\boldsymbol{\theta}'$  satisfying the following three conditions:

(i) local-in-layer condition: weights of each layer in NN' are inherited from NN except for layer  $\hat{q}$  and  $q+1$ , i.e.,

$$\begin{cases} \boldsymbol{\theta}'|_l = \boldsymbol{\theta}|_l, & \text{for } l \in [q] \cup [q+2 : L], \\ \boldsymbol{\theta}'|_{\hat{q}} = (\mathbf{W}'^{[\hat{q}]}, \mathbf{b}'^{[\hat{q}]}) \in \mathbb{R}^{m'_{\hat{q}} \times m'_{\hat{q}-1}} \times \mathbb{R}^{m'_{\hat{q}}}, \\ \boldsymbol{\theta}'|_{q+1} = (\mathbf{W}'^{[q+1]}, \mathbf{b}'^{[q+1]}) \in \mathbb{R}^{m'_{q+1} \times m'_{\hat{q}}} \times \mathbb{R}^{m'_{q+1}}, \end{cases}$$

(ii) layer linearization condition: for any  $j \in [m'_{\hat{q}}]$ , there exists an affine subdomain  $(a_j, b_j)$  of  $\sigma$  associated with  $\lambda_j, \mu_j$  such that the  $j$ -th component  $(\mathbf{W}'^{[\hat{q}]} \mathbf{f}_{\boldsymbol{\theta}'}^{[q]}(\mathbf{x}) + \mathbf{b}'^{[\hat{q}]})_j \in (a_j, b_j)$  for any  $\mathbf{x} \in S_{\mathbf{x}}$ .

(iii) output preserving condition:

$$\begin{cases} \mathbf{W}'^{[q+1]} \text{diag}(\boldsymbol{\lambda}) \mathbf{W}'^{[\hat{q}]} = \mathbf{W}^{[q+1]}, \\ \mathbf{W}'^{[q+1]} \text{diag}(\boldsymbol{\lambda}) \mathbf{b}'^{[\hat{q}]} + \mathbf{W}'^{[q+1]} \boldsymbol{\mu} + \mathbf{b}'^{[q+1]} = \mathbf{b}^{[q+1]}, \end{cases}$$

where  $\boldsymbol{\lambda} = [\lambda_1, \lambda_2, \dots, \lambda_{m'_{\hat{q}}}]^{\top} \in \mathbb{R}^{m'_{\hat{q}}}$ ,  $\boldsymbol{\mu} = [\mu_1, \mu_2, \dots, \mu_{m'_{\hat{q}}}]^{\top} \in \mathbb{R}^{m'_{\hat{q}}}$ .

**Remark.** Here we misuse the manifold to include any finite union of manifolds. Intuitively, above operator maps a point  $\boldsymbol{\theta}$  of NN to a manifold in a higher dimensional Euclidean space. We name it the one-layer lifting because it can be regarded as a lifting from a point in the base space to a "fiber". In turn, the inverse of one-layer lifting is a projection, which projects the parameter space of a deep NN to the parameter space of a shallower NN.

As shown in Fig. 2, a one-layer lifting is performed by inserting a hidden layer, say the pink layer ( $\hat{q}$ -th layer) in the right network. Value of the one-layer lifting is a subset/manifold of the parameter space of the right network consisting of each parameter vector satisfying the following constraints. The parameters  $\mathbf{W}'^{[\hat{q}]}, \mathbf{b}'^{[\hat{q}]}$  of the inserted layer satisfy the layer linearization condition such that this layer behaves like a linear layer on the training inputs. And the parameters  $\mathbf{W}'^{[q+1]}, \mathbf{b}'^{[q+1]}$  of  $(q+1)$ -th layer satisfy the output preserving condition such that the composition of the  $\hat{q}$ -th layer

and  $(q + 1)$ -th layer in the right network is equivalent to the  $(q + 1)$ -th layer in the left network.

Because factorized weights satisfying both layer linearization and output preserving conditions always exist, we have the following existence result for one-layer lifting.

**Lemma 1 (existence of one-layer lifting).** (see Appendix A: Lem. 1 for proof) Given data  $S$ , any  $\text{NN}(\{m_l\}_{l=0}^L)$  and a one-layer deeper  $\text{NN}'(\{m'_l\}, l \in \{0, 1, 2, \dots, q, \hat{q}, q + 1, \dots, L\})$ , the one-layer lifting  $\mathcal{T}_S$  exists, i.e.,  $\mathcal{T}_S(\theta_{\text{sh}})$  is not empty for any parameter  $\theta_{\text{sh}}$  of NN.

## 4.2 Embedding Principle in Depth

The multi-layer lifting is defined as a composition of multiple one-layer liftings. Then parameter of any NN can be lifted to a parameter manifold of any deeper NN through a multi-layer lifting. Both one-layer and multi-layer liftings possess the following properties.

**Proposition 1 (network properties preserving).** (see Appendix A: Prop. 1 for proof) Given any  $\text{NN}(\{m_l\}_{l=0}^L)$  and data  $S$ , for any one-layer lifting  $\mathcal{T}_S$  and any network parameter  $\theta_{\text{sh}}$  of NN, the following network properties are preserved for any  $\theta'_{\text{deep}} \in \mathcal{T}_S(\theta_{\text{sh}})$ :

(i) outputs are preserved:  $f_{\theta'_{\text{deep}}}(\mathbf{x}) = f_{\theta_{\text{sh}}}(\mathbf{x})$  for  $\mathbf{x} \in S_{\mathbf{x}}$ ;

(ii) empirical risk is preserved:  $R_S(\theta'_{\text{deep}}) = R_S(\theta_{\text{sh}})$ ;

(iii) the network representations are preserved for all layers:  $\text{span}\{\{(\mathbf{f}_{\theta'_{\text{deep}}}^{[q]}(\mathbf{X}))_j\}_{j \in [m'_q]} \cup \{\mathbf{1}\}\} = \text{span}\{\{(\mathbf{f}_{\theta_{\text{sh}}}^{[q]}(\mathbf{X}))_j\}_{j \in [m_q]} \cup \{\mathbf{1}\}\}$ , and for the other index  $l \in [L]$ ,  $\text{span}\{\{(\mathbf{f}_{\theta'_{\text{deep}}}^{[l]}(\mathbf{X}))_j\}_{j \in [m'_l]} \cup \{\mathbf{1}\}\} = \text{span}\{\{(\mathbf{f}_{\theta_{\text{sh}}}^{[l]}(\mathbf{X}))_j\}_{j \in [m_l]} \cup \{\mathbf{1}\}\}$ , where  $\mathbf{f}_{\theta}^{[l]}(\mathbf{X}) = [\mathbf{f}_{\theta}^{[l]}(\mathbf{x}_1), \mathbf{f}_{\theta}^{[l]}(\mathbf{x}_2), \dots, \mathbf{f}_{\theta}^{[l]}(\mathbf{x}_n)]^{\top} \in \mathbb{R}^{n \times m'_q}$  and  $\mathbf{1} \in \mathbb{R}^n$  is the all-ones vector.

**Proposition 2 (criticality preserving).** (see Appendix A: Prop. 2 for proof) Given any  $\text{NN}(\{m_l\}_{l=0}^L)$  and data  $S$ , for any one-layer lifting  $\mathcal{T}_S$ , if  $\theta_{\text{sh}}$  of NN satisfies  $\nabla_{\theta} R_S(\theta_{\text{sh}}) = \mathbf{0}$ , then  $\nabla_{\theta'} R_S(\theta'_{\text{deep}}) = \mathbf{0}$  for any  $\theta'_{\text{deep}} \in \mathcal{T}_S(\theta_{\text{sh}})$ .

Because of the criticality preserving property, we refer to one-layer or multi-layer lifting as *critical lifting*. Using above results, we now arrive at an embedding principle in depth as follows, which can be intuitively described as: *loss landscape of any DNN contains a hierarchy of critical manifolds lifted from all critical points of the loss landscapes for all shallower NNs.*

**Theorem 1 (embedding principle in depth).** (see Appendix A: Thm. 1 for proof) Given any  $\text{NN}'(\{m'_l\}_{l=0}^{L'})$  and data  $S$ , for any  $\theta_c$  of any shallower  $\text{NN}(\{m_l\}_{l=0}^L)$  satisfying  $\nabla_{\theta} R_S(\theta_c) = \mathbf{0}$ , there exists parameter  $\theta'_c$  in the loss landscape of  $\text{NN}'(\{m'_l\}_{l=0}^{L'})$  satisfying the following conditions:

(i)  $\mathbf{f}_{\theta'_c}(\mathbf{x}) = \mathbf{f}_{\theta_c}(\mathbf{x})$  for  $\mathbf{x} \in S_{\mathbf{x}}$ ;

(ii)  $\nabla_{\theta'} R_S(\theta'_c) = \mathbf{0}$ .

**Remark.** Although we only prove output preserving for training inputs, the NN output function is actually preserved over a broader area of input space including at least a neighbourhood of each training input (see Appendix A: Prop. 4 for proof). If the training dataset is sufficiently large and representative, then our lifting operator effectively preserves the generalization performance.

With the help of critical lifting, above embedding principle in depth provides a clear picture about the hierarchical structure of critical points/manifolds in depth in the loss landscape of a DNN. This hierarchical structure has a profound impact on the nonlinear training behavior of a deep network because any training trajectory nearby has a tendency to be attracted to these points/manifolds. Note that, the critical lifting is data-dependent. Its data-dependence is characterized by the following proposition.

**Proposition 3 (data dependency of critical lifting).** (see Appendix A: Prop. 3 for proof) Given any  $\text{NN}(\{m_l\}_{l=0}^L)$  and data  $S$ , for any critical lifting  $\mathcal{T}_S$  and any parameter  $\theta_{\text{sh}}$  of NN, if data  $S' \subseteq S$ , then  $\mathcal{T}_S(\theta_{\text{sh}}) \subseteq \mathcal{T}_{S'}(\theta_{\text{sh}})$ .

This result shows that increasing training data shrinks any lifted manifold to its subset. It informs us that increasing training data is an effective way to reduce the lifted critical manifolds, and can lead to a faster decay of training loss demonstrated in the following experimental study.

## 5 Experiments: Practical Implications

The embedding principle in depth provides new understandings to many widely observed behaviors of DNNs. We first briefly introduce our experimental setup, and then present our experimental results.

### 5.1 Experimental Setup

Throughout this work, we use fully-connected NNs. The input dimension  $d$  and output dimension  $d'$  are determined by the training data. Each hidden layer has the same width  $m$ . All parameters are initialized by a Gaussian distribution with mean zero and variance specified in each experiment. We use MSE loss for regression and cross-entropy loss for classification trained by gradient descent. The learning rate is fixed throughout the training. The batch normalization normalizes the layers' inputs by re-centering and re-scaling:  $\text{BN}(\mathbf{x}) = \gamma \circ \frac{\mathbf{x} - \hat{\mu}_B}{\hat{\sigma}_B} + \beta$  with a default initialization  $\gamma = 1, \beta = 0$ . More details of experiments are presented in Appendix C of Supplements.

**Measuring layer linearization by Minimal Pearson Correlation (MPC).** For the detection of lifted critical points in experiments, we propose the following method to measure their key feature, i.e., layer linearization. Let  $\tilde{\mathbf{f}}_{\theta}^{[l]} = \mathbf{W}^{[l]} \mathbf{f}_{\theta}^{[l-1]} + \mathbf{b}^{[l]} \in \mathbb{R}^{m_l}$  and  $\mathbf{f}_{\theta}^{[l]} = \sigma(\tilde{\mathbf{f}}_{\theta}^{[l]}) \in \mathbb{R}^{m_l}$  denote the input and output of neurons in layer  $l$ , respectively. For each neuron in a layer, the absolute value of the Pearson correlation coefficient is used to measure the extent of linearization for each neuron. By taking the minimum over the whole layer, we obtain the following measure of the extent

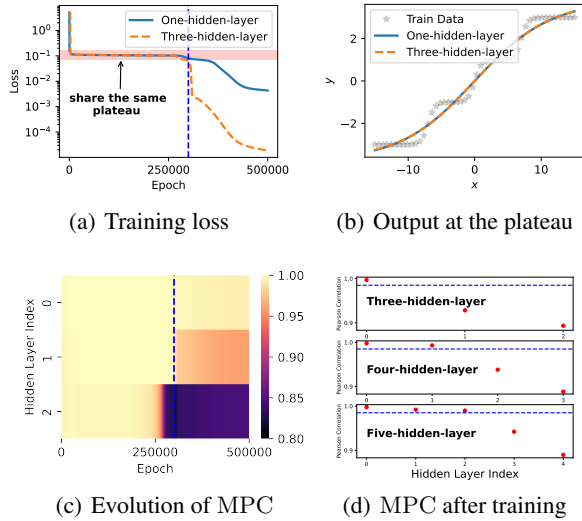


Figure 3: (a) The training loss for single-hidden-layer and three-hidden-layer NNs with width  $m = 50$ . (b) The outputs of NNs with different depths at the same loss value indicated by the colored span in (a). (c) The extent of layer linearization for different hidden layers during the training process of the three-hidden-layer NN. (d) The MPC of NNs with different depth after training (loss  $< 10^{-3}$ ). The auxiliary dash line is  $y = 0.99$ .

of linearization for the  $l$ -th layer, i.e.,

$$\text{MPC}(\mathbf{f}_\theta^{[l]}, \tilde{\mathbf{f}}_\theta^{[l]}) = \min_{j \in [m_l]} |\rho((\mathbf{f}_\theta^{[l]})_j, (\tilde{\mathbf{f}}_\theta^{[l]})_j)| \in [0, 1], \quad (1)$$

where  $(\mathbf{f}_\theta^{[l]})_j, (\tilde{\mathbf{f}}_\theta^{[l]})_j$  are the  $j$ -th components of  $\mathbf{f}_\theta^{[l]}$  and  $\tilde{\mathbf{f}}_\theta^{[l]}$ , respectively, and  $\rho((\mathbf{f}_\theta^{[l]})_j, (\tilde{\mathbf{f}}_\theta^{[l]})_j)$  is the Pearson correlation coefficient.

## 5.2 Practical Implications

In this subsection, we first show that the lifted critical points can be experienced during the training and then demonstrate the implications of the embedding principle in depth to various training behaviors as well as the layer pruning of DNNs.

**Deep NNs experience lifted critical points.** We train tanh NNs of different depths (width  $m = 50$ ) to learn the data shown in Fig. 3(b) and trace the evolution of MPC of each hidden layer computed by Eq. (1). As shown in Fig. 3(a), the three-hidden-layer NN first stagnates at the same loss value as the single-hidden-layer NN with almost the same output function in Fig. 3(b). From Fig. 3(c), the first two hidden layers exhibit strong linearity at stagnation. We further verify that the critical point experienced by three-hidden-layer NN is lifted from a single-hidden-layer NN through merging the effectively linear layers to a critical point of the single-hidden-layer NN (see Appendix B Fig. B1). By calculating the MPC after training (loss  $< 10^{-3}$ ), we observe that when the depth of the NN continues to increase

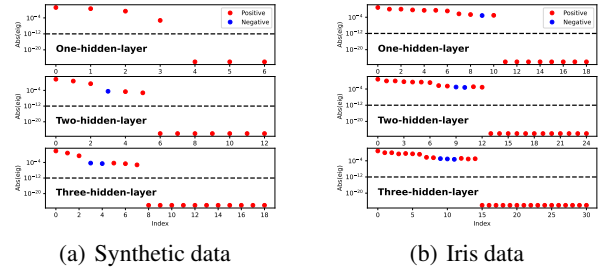


Figure 4: Eigenvalues of Hessian of NNs at the critical points lifted from the NN with single hidden layer for learning data of Fig. 3(b) in (a) and for Iris dataset in (b). The auxiliary dash line in each sub-figure is  $y = 10^{-12}$ . We do the lifting operation by factorizing one hidden layer into  $k$  hidden layers ( $k = 2, 3$ ), whose input weights are identity and biases are selected to translate the input range into the non-constant linear segment of ReLU.

beyond the necessary depth, the number of effectively linear layers (MPC  $> 0.99$ ) also increases, e.g., from 1 to 2 to 3 in Fig. 3(d). This phenomenon implies a potential implicit bias of DNN towards a shallower fitting, which could contribute to the generalization of deep NNs. Similar phenomenon can be observed for ReLU NNs and residual NNs (see Appendix B Figs. B2 and B3).

**Transition to strict saddle points through lifting.** We train a single-hidden-layer ReLU NN with width  $m = 2$  to learn data of Fig. 3(b) shown in Fig. 4(a) or Iris dataset in Fig. 4(b) to a critical point (the  $L_1$  norm of gradient less than  $10^{-4}$ ). We then lift this critical point through a one-layer lifting and a two-layer lifting to NNs of 2 hidden layers and 3 hidden layers with each hidden layer the same width, respectively. In Fig. 4(a), for width-2 single-hidden-layer NN, all eigenvalues of Hessian are greater than or equal to 0 indicating a local minimum or non-strict saddle, which is hard to escape. After lifting, it becomes a strict saddle due to the emergence of negative eigenvalues (blue). Specifically, in both Fig. 4(a) and (b), we observe a steady increase of significant negative eigenvalues, e.g., from 0 to 1 to 2 in Fig. 4(a) and from 1 to 2 to 3 in Fig. 4(b). This minimum-to-saddle transition can also be observed in tanh NNs (see Appendix B Fig. B4). These observations imply a reduced difficulty in escaping lifted critical points in deeper NNs, which provides new insight to the training efficiency of deep networks.

**Batch normalization avoids lifted critical points.** Empirically, using BN can greatly speed up NN training. Intuitively, BN enhances the expression of nonlinearity of each neuron, thus can well suppress layer linearization. As embedding principle in depth unravels a large family of lifted critical points with layer linearization, avoiding these critical points through suppressing layer linearization may be an important mechanism underlying the training efficiency of BN in practice. To verify this mechanism, we perform the following experiment shown in Fig. 5. We train a 2-hidden-layer tanh NN (width  $m = 50$ ) to learn the data in Fig. 3(b),

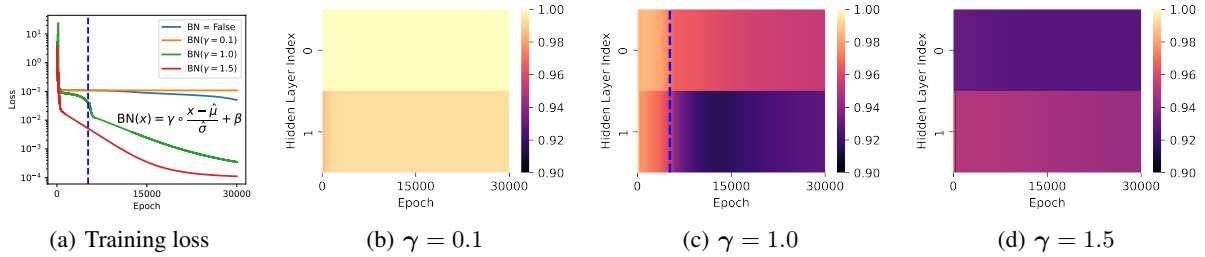


Figure 5: (a) Trajectories of training loss without BN and with BN of different initial values. (b, c, d) The extent of layer linearization for all hidden layers with BN of scaling parameter  $\gamma$  initialized at 0.1, 1.0, or 1.5, respectively. The auxiliary dash lines in (a) and (c) correspond to the same epoch.

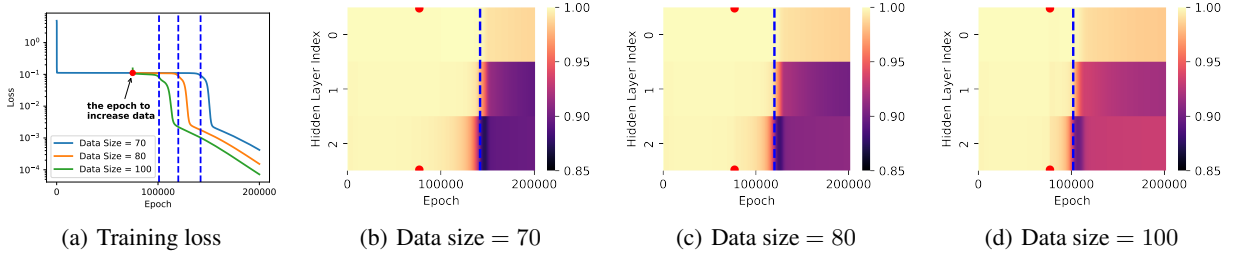


Figure 6: (a) The training loss of three-hidden-layer NN with width  $m = 50$  for learning data of Fig. 3(b). We sample 70, 80 and 100 data points equally spaced around 0, respectively. The red point in (a) is selected for switching dataset. (b, c, d) The extent of layer linearization for all hidden layers on datasets of different size, respectively. The red points correspond to the epoch to switch dataset. The auxiliary dash lines correspond to the epoch where NNs escape from the lifted critical point.

and compare the training trajectories without BN and with BN of scaling parameter  $\gamma$  initialized at 0.1, 1.0, or 1.5. Conforming with our intuition, a larger  $\gamma$  better suppresses layer linearization throughout the training as shown in Fig. 5(b)-(d). Moreover, the stagnation is significantly alleviated with a larger  $\gamma$ . There is even no stagnation for  $\gamma$  initialized at 1.5, signifying complete avoidance of lifted critical points as predicted by above mechanism.

**Optimization benefit of large dataset.** Prop. 3 characterizes the data dependency of critical lifting. The intuition is that larger dataset adds to the difficulty of layer linearization and thus helps reduce the critical manifolds. This result provides a seemingly counter-intuitive prediction that larger dataset may be more easily fitted due to the reduced critical manifolds lifted from shallower NNs. This prediction is verified by the following experiment in Fig. 6. We train a tanh NN with 3 hidden layers (width  $m = 50$ ) to learn data (data size  $n = 70$ ) of Fig. 3(b) to a critical point (the red point in Fig. 6(a)). We then continue (blue curve) or switch to larger datasets (orange and green curves) for training. As shown in Fig. 6(a), more training data leads to faster escape from the lifted critical point. Fig. 6(b-d) further trace the extent of layer linearization for each hidden layer on datasets of different sizes, respectively. From Fig. 6(c-d), we can clearly see that more data facilitate the expression of nonlinearity of hidden layers (see the abrupt reductions of MPC at the red dot) so as to help escape the critical point lifted from a

single-hidden-layer NN as implied by Prop. 3.

**Layer pruning of DNN with layer linearization.** The embedding principle in depth predicts a family of critical points with layer linearization. These critical points intrinsically come from shallower NNs, thus possessing good layer pruning potential. To realize such pruning potential in practice, we propose the method of detecting and merging effectively linear layers, which works as follows. We train a deep 10-hidden-layer tanh NN (width  $m = 50$ ) on the MNIST dataset. At the red dot in Fig. 7(a), the training loss decreases very slowly, presumably is very close to a global minimum. As shown in Fig. 7(b), there are 5 effective linear layers (MPC > 0.99) at this point. We merge these effective linear layers by properly multiplying their weights, thereby pruning the NN of 10 hidden layers to 5 hidden layers. The parameters before reduction is denoted by  $\theta_{\text{ori}}$  and after reduction by  $\theta_{\text{redu}}$ . We further train the pruned NN from  $\theta_{\text{redu}}$  as shown in Fig. 7(c) which quickly fall into the same loss value as the red point in Fig. 7(a). We then compare the prediction between original model and the pruned model at the corresponding red point on 10000 test data as shown in Fig. 7(d). Although our critical lifting does not preserve the output function over the entire domain of input, we still observe well agreement of these two models (overall  $\sim 98.54\%$ ), which implies that this reduction can approximately preserve the generalization performance (95.4% to 95.27%).

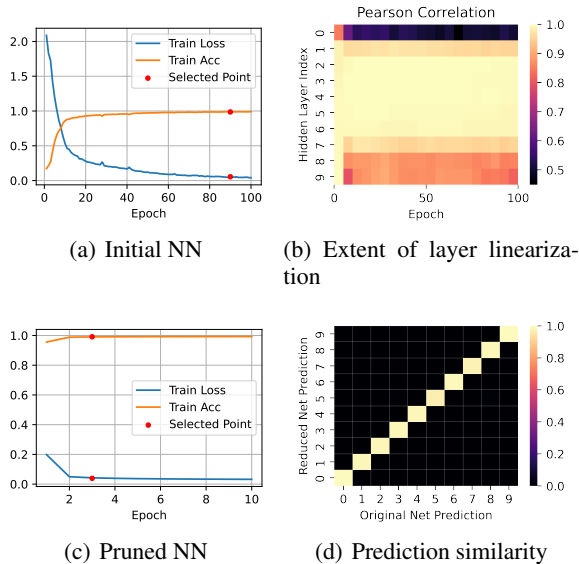


Figure 7: (a) The training process of the original 10-hidden-layer network on MNIST dataset. The red dot is selected for layer pruning. (b) The extent of layer linearization for all hidden layers. (c) The training process after layer pruning. (d) Prediction similarity between initial and reduced network on the test dataset. For each grid, color indicates the ratio of that prediction pair  $(i, j)$  over all samples predicted as  $j$  by the original 10-hidden-layer NN.

## 6 Discussion

### 6.1 Differences Between Embedding Principle in Width and in Depth

Our work is inspired by the embedding principle in width (Zhang et al. 2021b) and for the first time addresses the embedding relation in depth for DNNs. Though our critical lifting operator shares the same spirit of the critical embedding operator in Zhang et al. (2021b), there are several distinctions listed as follows.

(i) **The target NN.** The critical lifting maps to the parameter space of a deeper NN whereas the critical embedding maps to the parameter space of a wider NN.

(ii) **The requirement for activation function.** The critical lifting requires a layer linearization condition, which can be satisfied for any activation with a non-constant linear segment, e.g., ReLU, leaky-ReLU and ELU, and approximately satisfied for general smooth activations, e.g., sigmoid, tanh and gelu. However, the critical embedding works for general activation function.

(iii) **The type of mapping.** The critical lifting is a set-valued function which maps any parameter vector to a manifold, whereas the critical embedding is a vector-valued function.

(iv) **The output preserving property.** The critical lifting preserves the DNN outputs at the training dataset, whereas the critical embedding preserves the DNN output function over the whole input domain.

(v) **The data dependency.** The critical lifting is data-dependent, whereas the embedding operator is independent on data. For critical lifting, we prove that more data leads to reduced lifted manifolds in Prop. 3. In contrast, the critical embedding is data-independent.

The key distinctions (iii)-(v) originate from the intrinsically different expressiveness between adding width and adding depth of a DNN, i.e., the function space of a narrow NN is strictly a subset of the function space of any wider NN (see Fukumizu et al. (2019); Zhang et al. (2021b)) whereas a similar (embedding) relation about the expressiveness can only be expected in the sense of approximation in general regarding shallow and deeper NNs.

### 6.2 Other Network Architectures

The embedding principle in depth results from the layer stacking nature of deep neural networks, in which each layer can be linearly factorized into multiple layers. Therefore, our theoretical results proved for fully-connected DNNs can be naturally extended to other NN architectures such as convolutional neural networks and residual networks. For example, for a residual network, the only change needed to obtain its one-layer lifting operator is to modify the output preserving condition (see Appendix A: Def. 2 for details).

Note that for residual networks, simply choosing the parameters of the inserted block to be zero is a trivial criticality preserving lifting, which automatically satisfies the layer linearization condition. However, we must point out that whether the lifted critical points can be experienced in practice determines the importance of different liftings. In fact, as shown in Fig. B3 of Appendix B, we rarely observe such trivially lifted critical points. In contrast, the proposed lifted critical points with layer linearization can often be observed in experiments. Therefore, the critical lifting operator proposed in this work is of special value for studying the training behavior of DNNs in practice.

### 6.3 Simplicity Bias

Our embedding principle in depth combined with the previous embedding principle in width explicitly characterizes the hierarchical structure of DNN loss landscape in both width and depth. This hierarchical structure highlights the non-overfitting potential even when a very large NN is used to fit limited training data generated by a much smaller (i.e., shallower and narrower) NN. The intuition is that, guided by the hierarchy of “simple” critical points/manifolds lifted/embedded from narrower and shallower NNs, a large NN may learn a “simple” interpolation from a small NN through training. This potential is further supported by our numerical experiments in Figs. 3, 5, 6 and 7 that the “effective” depth, i.e., number of nonlinear layers, often gradually increases during the training of deep NNs. It is tempting to conjecture that, with proper initialization, a large DNN could adaptively increase its “effective” depth and width based on the complexity of training data. We will examine this conjecture in our future works.

## 7 Conclusion

We discover an embedding principle in depth that loss landscape of a deep NN inherits all critical points for shallower NNs. We propose the critical lifting operator that proves and provides details about this principle. We also empirically demonstrate the rich insights provided by this principle to easy optimization of deep networks, acceleration effect of batch normalization and large dataset, as well as layer pruning. Note that, experiments in this work serve as proofs of concept for these new insights. Further systematical experimental studies are needed to fully understand the practical significance of these insights.

Overall, our discovery of the embedding principle in depth together with the previous embedding principle in width provides a complete picture about the intrinsic hierarchical structure of the DNN loss landscape. This picture firmly supports the empirically observed training and generalization similarity between NNs of different sizes, shedding light on the non-overfitting mystery of large NNs.

## Acknowledgments

This work is sponsored by the National Key R&D Program of China Grant No. 2019 YFA0709503 (Z. X.), the Shanghai Sailing Program, the Natural Science Foundation of Shanghai Grant No. 20ZR1429000 (Z. X.), the National Natural Science Foundation of China Grant No. 62002221 (Z. X.), the National Natural Science Foundation of China Grant No. 12101401 (T. L.), the National Natural Science Foundation of China Grant No. 12101402 (Y. Z.), Shanghai Municipal of Science and Technology Project Grant No. 20JC1419500 (Y.Z.), Shanghai Municipal of Science and Technology Major Project No. 2021SHZDZX0102, the Lingang Laboratory Grant No. LG-QS-202202-08, and the HPC of School of Mathematical Sciences and the Student Innovation Center at Shanghai Jiao Tong University.

## References

Arora, S.; Cohen, N.; and Hazan, E. 2018. On the optimization of deep networks: Implicit acceleration by overparameterization. In *International Conference on Machine Learning*, 244–253. PMLR.

Ba, J.; and Caruana, R. 2014. Do deep nets really need to be deep? *Advances in neural information processing systems*, 27.

Breiman, L. 1995. Reflections after refereeing papers for NIPS. *The Mathematics of Generalization*, XX: 11–15.

Cheridito, P.; Jentzen, A.; and Rossmannek, F. 2021. Landscape analysis for shallow ReLU neural networks: complete classification of critical points for affine target functions. *arXiv preprint arXiv:2103.10922*.

Du, S.; and Lee, J. 2018. On the power of overparameterization in neural networks with quadratic activation. In *International Conference on Machine Learning*, 1329–1338. PMLR.

E, W.; and Qingcan, W. 2018. Exponential convergence of the deep neural network approximation for analytic functions. *SCIENCE CHINA Mathematics*, 61(10): 1733.

Eldan, R.; and Shamir, O. 2016. The power of depth for feedforward neural networks. In *Conference on learning theory*, 907–940.

Fisher, R. A. 1936. The use of multiple measurements in taxonomic problems. *Annals of eugenics*, 7(2): 179–188.

Fukumizu, K.; and Amari, S.-i. 2000. Local minima and plateaus in hierarchical structures of multilayer perceptrons. *Neural networks*, 13(3): 317–327.

Fukumizu, K.; Yamaguchi, S.; Mototake, Y.-i.; and Tanaka, M. 2019. Semi-flat minima and saddle points by embedding neural networks to overparameterization. *Advances in Neural Information Processing Systems*, 32: 13868–13876.

He, H.; Huang, G.; and Yuan, Y. 2019. Asymmetric valleys: Beyond sharp and flat local minima. *arXiv preprint arXiv:1902.00744*.

He, K.; Zhang, X.; Ren, S.; and Sun, J. 2016. Deep residual learning for image recognition. In *Proceedings of the IEEE conference on computer vision and pattern recognition*, 770–778.

Ioffe, S.; and Szegedy, C. 2015. Batch normalization: Accelerating deep network training by reducing internal covariate shift. In *International conference on machine learning*, 448–456. PMLR.

Keskar, N. S.; Nocedal, J.; Tang, P. T. P.; Mudigere, D.; and Smelyanskiy, M. 2017. On large-batch training for deep learning: Generalization gap and sharp minima. In *5th International Conference on Learning Representations, ICLR 2017*.

Lee, J. D.; Panageas, I.; Piliouras, G.; Simchowitz, M.; Jordan, M. I.; and Recht, B. 2019. First-order methods almost always avoid strict saddle points. *Mathematical programming*, 176(1): 311–337.

Rahaman, N.; Arpit, D.; Baratin, A.; Draxler, F.; Lin, M.; Hamprecht, F. A.; Bengio, Y.; and Courville, A. 2019. On the Spectral Bias of Deep Neural Networks. *International Conference on Machine Learning*.

Romero, A.; Ballas, N.; Kahou, S. E.; Chassang, A.; Gatta, C.; and Bengio, Y. 2015. FitNets: Hints for Thin Deep Nets. In *ICLR (Poster)*.

Simsek, B.; Ged, F.; Jacot, A.; Spadaro, F.; Hongler, C.; Gerstner, W.; and Brea, J. 2021. Geometry of the Loss Landscape in Overparameterized Neural Networks: Symmetries and Invariances. In *Proceedings of the 38th International Conference on Machine Learning*, 9722–9732. PMLR.

Skorokhodov, I.; and Burtsev, M. 2019. Loss landscape sightseeing with multi-point optimization. *arXiv preprint arXiv:1910.03867*.

Soltanolkotabi, M.; Javanmard, A.; and Lee, J. D. 2018. Theoretical insights into the optimization landscape of overparameterized shallow neural networks. *IEEE Transactions on Information Theory*, 65(2): 742–769.

Telgarsky, M. 2016. benefits of depth in neural networks. In *Conference on Learning Theory*, 1517–1539.

Wu, L.; Zhu, Z.; et al. 2017. Towards understanding generalization of deep learning: Perspective of loss landscapes. *arXiv preprint arXiv:1706.10239*.



Xu, Z. J.; and Zhou, H. 2021. Deep Frequency Principle Towards Understanding Why Deeper Learning Is Faster. In AAAI, 10541–10550. AAAI Press.

Xu, Z.-Q. J.; Zhang, Y.; Luo, T.; Xiao, Y.; and Ma, Z. 2020. Frequency principle: Fourier analysis sheds light on deep neural networks. *Communications in Computational Physics*, 28(5): 1746–1767.

Xu, Z.-Q. J.; Zhang, Y.; and Xiao, Y. 2019. Training behavior of deep neural network in frequency domain. *International Conference on Neural Information Processing*, 264–274.

Zhang, C.; Bengio, S.; Hardt, M.; Recht, B.; and Vinyals, O. 2017. Understanding deep learning requires rethinking generalization. In *5th International Conference on Learning Representations, ICLR 2017, Toulon, France, April 24-26, 2017, Conference Track Proceedings*. OpenReview.net.

Zhang, Y.; Li, Y.; Zhang, Z.; Luo, T.; and Xu, Z. J. 2022. Embedding Principle: A Hierarchical Structure of Loss Landscape of Deep Neural Networks. *Journal of Machine Learning*, 1(1): 60–113.

Zhang, Y.; Luo, T.; Ma, Z.; and Xu, Z.-Q. J. 2021a. A Linear Frequency Principle Model to Understand the Absence of Overfitting in Neural Networks. *Chinese Physics Letters*, 38(3): 038701.

Zhang, Y.; Zhang, Z.; Luo, T.; and Xu, Z. J. 2021b. Embedding principle of loss landscape of deep neural networks. *Advances in Neural Information Processing Systems*, 34: 14848–14859.

## Appendix A: Proofs

**Definition 4 (one-layer lifting).** Given training data  $S$ , an NN  $(\{m_l\}_{l=0}^L)$  and a one-layer deeper NN'  $(\{m'_l\}, l \in \{0, 1, 2, \dots, q, \hat{q}, q+1, \dots, L\})$ , suppose  $m'_1 = m_1, \dots, m'_q = m_q, m'_{q+1} = m_{q+1}, \dots, m'_L = m_L$ . The one-layer lifting  $\mathcal{T}_S$  maps any parameter  $\theta = (\mathbf{W}^{[1]}, \mathbf{b}^{[1]}, \dots, \mathbf{W}^{[L]}, \mathbf{b}^{[L]})$  of NN to a manifold  $\mathcal{M}(\mathcal{M} := \mathcal{T}_S(\theta))$  of NN's parameter space, where  $\mathcal{M}$  is a collection of all  $\theta'$  satisfying the following three conditions:

(i) local-in-layer condition: weights of each layer in NN' are inherited from NN except for layer  $\hat{q}$  and  $q+1$ , i.e.,

$$\begin{cases} \theta'_l = \theta_l, & \text{for } l \in [q] \cup [q+2 : L], \\ \theta'_{\hat{q}} = (\mathbf{W}'^{[\hat{q}]}, \mathbf{b}'^{[\hat{q}]}) \in \mathbb{R}^{m'_{\hat{q}} \times m'_{q-1}} \times \mathbb{R}^{m'_{\hat{q}}}, \\ \theta'_{q+1} = (\mathbf{W}'^{[q+1]}, \mathbf{b}'^{[q+1]}) \in \mathbb{R}^{m'_{q+1} \times m'_{\hat{q}}} \times \mathbb{R}^{m'_{q+1}}, \end{cases}$$

(ii) layer linearization condition: for any  $j \in [m_{\hat{q}}]$ , there exists an affine subdomain  $(a_j, b_j)$  of  $\sigma$  associated with  $\lambda_j, \mu_j$  such that the  $j$ -th component  $(\mathbf{W}'^{[\hat{q}]} \mathbf{f}_{\theta'}^{[q]}(\mathbf{x}) + \mathbf{b}'^{[\hat{q}]})_j \in (a_j, b_j)$  for any  $\mathbf{x} \in S_{\mathbf{x}}$ .

(iii) output preserving condition:

$$\begin{cases} \mathbf{W}'^{[q+1]} \text{diag}(\lambda) \mathbf{W}'^{[\hat{q}]} = \mathbf{W}^{[q+1]}, \\ \mathbf{W}'^{[q+1]} \text{diag}(\lambda) \mathbf{b}'^{[\hat{q}]} + \mathbf{W}'^{[q+1]} \boldsymbol{\mu} + \mathbf{b}'^{[q+1]} = \mathbf{b}^{[q+1]}, \end{cases}$$

where  $\boldsymbol{\lambda} = [\lambda_1, \lambda_2, \dots, \lambda_{m_{\hat{q}}}]^\top \in \mathbb{R}^{m'_{\hat{q}}}$ ,  $\boldsymbol{\mu} = [\mu_1, \mu_2, \dots, \mu_{m_{\hat{q}}}]^\top \in \mathbb{R}^{m'_{\hat{q}}}$ .

**Lemma 2 (existence of one-layer lifting).** Given data  $S$ , any NN  $(\{m_l\}_{l=0}^L)$  and a one-layer deeper NN'  $(\{m'_l\}, l \in \{0, 1, 2, \dots, q, \hat{q}, q+1, \dots, L\})$ , the one-layer lifting  $\mathcal{T}_S$  exists, i.e.,  $\mathcal{T}_S(\theta_{\text{shal}})$  is not empty for any parameter  $\theta_{\text{shal}}$  of NN.

*Proof.* We prove this lemma by construction. From the definition of one-layer deeper, we know that  $m'_1 = m_1, \dots, m'_q = m_q, m'_{\hat{q}} \geq \min\{m_q, m_{q+1}\}, m'_{q+1} = m_{q+1}, \dots, m'_L = m_L$ . Without loss of generality, we assume the width of the inserted layer  $m'_{\hat{q}}$  is equal to  $\min\{m_q, m_{q+1}\}$ . Our construction can be easily extended to the case with a wider inserted layer by adding zero-neurons, i.e., neurons whose input and output weights are all zero.

For any parameter  $\theta_{\text{shal}} = (\mathbf{W}^{[1]}, \mathbf{b}^{[1]}, \dots, \mathbf{W}^{[L]}, \mathbf{b}^{[L]})$  of the NN, we construct a  $\theta'_{\text{deep}}$  in  $\mathcal{T}_S(\theta_{\text{shal}})$  as follows. Since the activation function  $\sigma$  has a non-constant linear segment, there exists an affine subdomain  $(a, b)$  associated with  $\lambda, \mu \in \mathbb{R}$  ( $\lambda \neq 0$ ) such that  $\sigma(x) = \lambda x + \mu$  for  $x \in (a, b)$ . Let  $[x_{\text{low}}, x_{\text{up}}] \subseteq (a, b)$  ( $x_{\text{low}} \neq x_{\text{up}}$ ) be a closed interval of the affine subdomain and  $\boldsymbol{\lambda} = \lambda \mathbf{1} \in \mathbb{R}^{m_{\hat{q}}}$ ,  $\boldsymbol{\mu} = \mu \mathbf{1} \in \mathbb{R}^{m_{\hat{q}}}$ , where  $\mathbf{1} \in \mathbb{R}^{m_{\hat{q}}}$  is the all-ones vector. Now we discuss in two cases:

(1)  $\min\{m_q, m_{q+1}\} = m_{q+1}$ .

Denote training data by  $S = \{(\mathbf{x}_i, \mathbf{y}_i)\}_{i=1}^n$  and  $\tilde{\mathbf{f}}_{\theta_{\text{shal}}}^{[q+1]} = \mathbf{W}^{[q+1]} \mathbf{f}_{\theta_{\text{shal}}}^{[q]} + \mathbf{b}^{[q+1]} \in \mathbb{R}^{m_{q+1}}$ ,

$$x_{\min} = \min_{i \in [n], j \in [m_{q+1}]} \{(\tilde{\mathbf{f}}_{\theta_{\text{shal}}}^{[q+1]}(\mathbf{x}_i))_j\},$$

$$x_{\max} = \max_{i \in [n], j \in [m_{q+1}]} \{(\tilde{\mathbf{f}}_{\theta_{\text{shal}}}^{[q+1]}(\mathbf{x}_i))_j\},$$

where  $(\tilde{\mathbf{f}}_{\theta_{\text{shal}}}^{[q+1]}(\mathbf{x}_i))_j$  is the  $j$ -th component of  $\tilde{\mathbf{f}}_{\theta_{\text{shal}}}^{[q+1]}(\mathbf{x}_i)$ .

Now we transform the input range  $[x_{\min}, x_{\max}]$  into the affine subdomain  $[a, b]$  of the activation function  $\sigma$  through an affine transformation. To this end, we further discuss in two cases:

(i) case 1:  $x_{\min} \neq x_{\max}$ .

Let  $\xi = \frac{x_{\text{up}} - x_{\text{low}}}{x_{\max} - x_{\min}} \in \mathbb{R}$ ,  $\mathbf{W}'^{[\hat{q}]} = \xi \mathbf{W}^{[q+1]} \in \mathbb{R}^{m_{\hat{q}} \times m_q}$  and  $\mathbf{b}'^{[\hat{q}]} = \xi \mathbf{b}^{[q+1]} + (x_{\text{low}} - \xi x_{\min}) \mathbf{1} \in \mathbb{R}^{m_{\hat{q}}}$ ,

where  $\mathbf{1}$  is the all-ones vector. And then we let  $\mathbf{W}'^{[q+1]} = \frac{1}{\lambda \xi} \mathbf{I}_d \in \mathbb{R}^{m_{q+1} \times m_{\hat{q}}}$ , where  $\mathbf{I}_d$  is the identity matrix, and  $\mathbf{b}'^{[q+1]} = \mathbf{b}^{[q+1]} - \mathbf{W}'^{[q+1]} \text{diag}(\boldsymbol{\lambda}) \mathbf{b}'^{[\hat{q}]} - \mathbf{W}'^{[q+1]} \boldsymbol{\mu} \in \mathbb{R}^{m_{q+1}}$ . Finally, we let  $\theta'_{\text{deep}} = (\mathbf{W}^{[1]}, \mathbf{b}^{[1]}, \dots, \mathbf{W}^{[q]}, \mathbf{b}^{[q]}, \mathbf{W}'^{[\hat{q}]}, \mathbf{b}'^{[\hat{q}]}, \mathbf{W}'^{[q+1]}, \mathbf{b}'^{[q+1]}, \dots, \mathbf{W}^{[L]}, \mathbf{b}^{[L]})$ . Now we verify that  $\theta'_{\text{deep}} \in \mathcal{T}_S(\theta_{\text{shal}})$ , i.e.,  $\theta'_{\text{deep}}$  satisfies the three conditions of one-layer lifting. Firstly, by the construction of  $\theta'_{\text{deep}}$ , the local-in-layer condition is satisfied automatically.

Next, for any  $j \in [m_{\hat{q}}]$ , there exists an affine subdomain  $(a, b)$  associated with  $\lambda, \mu$  such that the  $j$ -th component  $(\mathbf{W}'^{[\hat{q}]} \mathbf{f}_{\theta'_{\text{deep}}}^{[q]}(\mathbf{x}) + \mathbf{b}'^{[\hat{q}]})_j =$

$(\xi \mathbf{W}^{[q+1]} \mathbf{f}_{\theta_{\text{shal}}}^{[q]}(\mathbf{x}) + \xi \mathbf{b}^{[q+1]} + (x_{\text{low}} - \xi x_{\text{min}}) \mathbf{1})_j = (\xi \tilde{\mathbf{f}}_{\theta_{\text{shal}}}^{[q+1]} + (x_{\text{low}} - \xi x_{\text{min}}) \mathbf{1})_j \in (a, b)$  for any  $\mathbf{x} \in S_{\mathbf{x}}$ . Thus the layer linearization condition holds.

Finally, by direct calculation, the output preserving condition holds:

$$\begin{cases} \mathbf{W}'^{[q+1]} \text{diag}(\boldsymbol{\lambda}) \mathbf{W}'^{[q]} = \mathbf{W}^{[q+1]}, \\ \mathbf{W}'^{[q+1]} \text{diag}(\boldsymbol{\lambda}) \mathbf{b}'^{[q]} + \mathbf{W}'^{[q+1]} \boldsymbol{\mu} + \mathbf{b}'^{[q+1]} = \mathbf{b}^{[q+1]}. \end{cases}$$

Collecting the above results, we prove that  $\theta'_{\text{deep}} \in \mathcal{T}_S(\theta_{\text{shal}})$ , i.e.,  $\mathcal{T}_S(\theta_{\text{shal}})$  is not empty.

(ii) case 2:  $x_{\text{min}} = x_{\text{max}}$ .

The layer linearization condition can be easily satisfied because the inputs to each neuron remain a constant. Therefore, by setting  $\xi \neq 0$  to any nonzero constant, the above construction works for this case, i.e., the constructed  $\theta'_{\text{deep}} \in \mathcal{T}_S(\theta_{\text{shal}})$ .

(2)  $\min\{m_q, m_{q+1}\} = m_q$ .

Denote training data by  $S = \{(\mathbf{x}_i, \mathbf{y}_i)\}_{i=1}^n$  and

$$\begin{aligned} x_{\text{min}} &= \min_{i \in [n], j \in [m_q]} \{(\mathbf{f}_{\theta_{\text{shal}}}^{[q]}(\mathbf{x}_i))_j\}, \\ x_{\text{max}} &= \max_{i \in [n], j \in [m_q]} \{(\mathbf{f}_{\theta_{\text{shal}}}^{[q]}(\mathbf{x}_i))_j\}, \end{aligned}$$

where  $(\mathbf{f}_{\theta_{\text{shal}}}^{[q]}(\mathbf{x}_i))_j$  is the  $j$ -th component of  $\mathbf{f}_{\theta_{\text{shal}}}^{[q]}(\mathbf{x}_i)$ .

Also, we can transform the input range  $[x_{\text{min}}, x_{\text{max}}]$  into the affine subdomain  $[a, b]$  of the activation function  $\sigma$  through an affine transformation. To this end, we also further discuss in two cases:

(i) case 1:  $x_{\text{min}} \neq x_{\text{max}}$ .

Let  $\xi = \frac{x_{\text{up}} - x_{\text{low}}}{x_{\text{max}} - x_{\text{min}}} \in \mathbb{R}$ ,  $\mathbf{W}'^{[q]} = \xi \mathbf{I}_d \in \mathbb{R}^{m_{\hat{q}} \times m_{\hat{q}}}$  and  $\mathbf{b}'^{[q]} = (x_{\text{low}} - \xi x_{\text{min}}) \mathbf{1} \in \mathbb{R}^{m_{\hat{q}}}$ . And then we let  $\mathbf{W}'^{[q+1]} = \frac{1}{\lambda \xi} \mathbf{W}^{[q+1]} \in \mathbb{R}^{m_{q+1} \times m_{\hat{q}}}$ , and  $\mathbf{b}'^{[q+1]} = \mathbf{b}^{[q+1]} - \mathbf{W}'^{[q+1]} \text{diag}(\boldsymbol{\lambda}) \mathbf{b}'^{[q]} - \mathbf{W}'^{[q+1]} \boldsymbol{\mu} \in \mathbb{R}^{m_{q+1}}$ . Finally, we set  $\theta'_{\text{deep}} = (\mathbf{W}^{[1]}, \mathbf{b}^{[1]}, \dots, \mathbf{W}^{[q]}, \mathbf{b}^{[q]}, \mathbf{W}'^{[q]}, \mathbf{b}'^{[q]}, \mathbf{W}'^{[q+1]}, \mathbf{b}'^{[q+1]}, \dots, \mathbf{W}^{[L]}, \mathbf{b}^{[L]})$ . We can verify that  $\theta'_{\text{deep}} \in \mathcal{T}_S(\theta_{\text{shal}})$  similar to the previous case 1.

(ii) case 2:  $x_{\text{min}} = x_{\text{max}}$ .

By setting  $\xi \neq 0$  to any nonzero constant, the above construction also works for this case, i.e., the constructed  $\theta'_{\text{deep}} \in \mathcal{T}_S(\theta_{\text{shal}})$ .

Therefore,  $\mathcal{T}_S(\theta_{\text{shal}})$  is non-empty for any  $\theta_{\text{shal}}$ , i.e., one-layer lifting exists.  $\square$

To prove the following Propositions 1 and 2, we first define some notations and prove a lemma.

For each  $l \in [L]$ , we define the error vectors  $\mathbf{z}_{\theta}^{[l]} = \nabla_{\mathbf{f}^{[l]}} \ell$  and the feature gradients  $\mathbf{g}_{\theta}^{[L]} = \mathbf{1}$  and  $\mathbf{g}_{\theta}^{[l]} = \sigma^{(1)}(\mathbf{W}^{[l]} \mathbf{f}_{\theta}^{[l-1]} + \mathbf{b}^{[l]})$  for  $l \in [L-1]$ , where  $\sigma^{(1)}$  is the first derivative of  $\sigma$ . Moreover, we call  $\mathbf{f}_{\theta}^{[l]}$ ,  $l \in [L]$  feature vectors and denote the collections of feature vectors,

feature gradients, and error vectors respectively by  $\mathbf{F}_{\theta} = \{\mathbf{f}_{\theta}^{[l]}\}_{l=1}^L$ ,  $\mathbf{G}_{\theta} = \{\mathbf{g}_{\theta}^{[l]}\}_{l=1}^L$ ,  $\mathbf{Z}_{\theta} = \{\mathbf{z}_{\theta}^{[l]}\}_{l=1}^L$ . Using back-propagation, we can calculate the gradients as follows

$$\begin{cases} \mathbf{z}_{\theta}^{[L]} = \nabla \ell, \\ \mathbf{z}_{\theta}^{[l]} = (\mathbf{W}^{[l+1]})^{\top} (\mathbf{z}_{\theta}^{[l+1]} \circ \mathbf{g}_{\theta}^{[l+1]}), \quad l \in [L-1], \\ \nabla_{\mathbf{W}^{[l]}} \ell = (\mathbf{z}_{\theta}^{[l]} \circ \mathbf{g}_{\theta}^{[l]}) (\mathbf{f}_{\theta}^{[l-1]})^{\top}, \quad l \in [L], \\ \nabla_{\mathbf{b}^{[l]}} \ell = \mathbf{z}_{\theta}^{[l]} \circ \mathbf{g}_{\theta}^{[l]}, \quad l \in [L]. \end{cases}$$

Now we prove the following lemma, of which Proposition 1 is a direct consequence.

**Lemma 3.** *Given data  $S$  and any NN  $(\{m_l\}_{l=0}^L)$ , for any one-layer lifting  $\mathcal{T}_S$  and any parameter  $\theta_{\text{shal}}$  of NN, we have  $\theta'_{\text{deep}} \in \mathcal{T}_S(\theta_{\text{shal}})$  satisfying the following conditions: there exist  $\boldsymbol{\lambda}, \boldsymbol{\mu} \in \mathbb{R}^{m_{\hat{q}}}$  such that for any  $\mathbf{x} \in S_{\mathbf{x}}$ , we have*

(i) *feature vectors in  $\mathbf{F}_{\theta'_{\text{deep}}}$ :  $\mathbf{f}_{\theta'_{\text{deep}}}^{[l]}(\mathbf{x}) = \mathbf{f}_{\theta_{\text{shal}}}^{[l]}(\mathbf{x})$  for  $l \in [L]$  and  $\mathbf{f}_{\theta'_{\text{deep}}}^{[q]}(\mathbf{x}) = \text{diag}(\boldsymbol{\lambda}) (\mathbf{W}'^{[q]} \mathbf{f}_{\theta_{\text{shal}}}^{[q]}(\mathbf{x}) + \mathbf{b}'^{[q]}) + \boldsymbol{\mu}$ ;*

(ii) *feature gradients in  $\mathbf{G}_{\theta'_{\text{deep}}}$ :  $\mathbf{g}_{\theta'_{\text{deep}}}^{[l]}(\mathbf{x}) = \mathbf{g}_{\theta_{\text{shal}}}^{[l]}(\mathbf{x})$  for  $l \in [L]$  and  $\mathbf{g}_{\theta'_{\text{deep}}}^{[q]}(\mathbf{x}) = \boldsymbol{\lambda}$ ;*

(iii) *error vectors in  $\mathbf{Z}_{\theta'_{\text{deep}}}$ :  $\mathbf{z}_{\theta'_{\text{deep}}}^{[l]}(\mathbf{x}) = \mathbf{z}_{\theta_{\text{shal}}}^{[l]}(\mathbf{x})$  for  $l \in [q-1] \cup [q+1 : L]$  and  $\mathbf{z}_{\theta'_{\text{deep}}}^{[q]}(\mathbf{x}) = (\mathbf{W}'^{[q+1]})^{\top} (\mathbf{z}_{\theta_{\text{shal}}}^{[q+1]}(\mathbf{x}) \circ \mathbf{g}_{\theta_{\text{shal}}}^{[q+1]}(\mathbf{x}))$ ,  $\mathbf{z}_{\theta'_{\text{deep}}}^{[q]}(\mathbf{x}) = (\mathbf{W}'^{[q]})^{\top} (\mathbf{z}_{\theta_{\text{shal}}}^{[q]}(\mathbf{x}) \circ \boldsymbol{\lambda})$ .*

*Proof.* (i) By the construction of  $\theta'_{\text{deep}}$ , it is clear that  $\mathbf{f}_{\theta'_{\text{deep}}}^{[l]}(\mathbf{x}) = \mathbf{f}_{\theta_{\text{shal}}}^{[l]}(\mathbf{x})$  for any  $l \in [q]$ . And by the definition of one-layer lifting, layer linearization condition is satisfied, i.e., for any  $j \in [m_{\hat{q}}]$ , there exists an affine subdomain  $(a_j, b_j)$  associated with  $\lambda_j, \mu_j$  such that the  $j$ -th component  $(\mathbf{W}'^{[q]} \mathbf{f}_{\theta_{\text{shal}}}^{[q]}(\mathbf{x}) + \mathbf{b}'^{[q]})_j \in (a_j, b_j)$  for any  $\mathbf{x} \in S_{\mathbf{x}}$ .

Therefore, there exist  $\boldsymbol{\lambda} = [\lambda_1, \lambda_2, \dots, \lambda_{m_{\hat{q}}}]^{\top} \in \mathbb{R}^{m_{\hat{q}}}$ ,  $\boldsymbol{\mu} = [\mu_1, \mu_2, \dots, \mu_{m_{\hat{q}}}]^{\top} \in \mathbb{R}^{m_{\hat{q}}}$  such that for any  $\mathbf{x} \in S_{\mathbf{x}}$

$$\begin{aligned} \mathbf{f}_{\theta'_{\text{deep}}}^{[q]}(\mathbf{x}) &= \sigma(\mathbf{W}'^{[q]} \mathbf{f}_{\theta_{\text{shal}}}^{[q]}(\mathbf{x}) + \mathbf{b}'^{[q]}) \\ &= \boldsymbol{\lambda} \circ (\mathbf{W}'^{[q]} \mathbf{f}_{\theta_{\text{shal}}}^{[q]}(\mathbf{x}) + \mathbf{b}'^{[q]}) + \boldsymbol{\mu} \\ &= \boldsymbol{\lambda} \circ (\mathbf{W}'^{[q]} \mathbf{f}_{\theta_{\text{shal}}}^{[q]}(\mathbf{x}) + \mathbf{b}'^{[q]}) + \boldsymbol{\mu} \\ &= \text{diag}(\boldsymbol{\lambda}) (\mathbf{W}'^{[q]} \mathbf{f}_{\theta_{\text{shal}}}^{[q]}(\mathbf{x}) + \mathbf{b}'^{[q]}) + \boldsymbol{\mu}. \end{aligned}$$

By the forward propagation process and the output preserving condition of one-layer lifting, we have

$$\begin{aligned} \mathbf{f}_{\theta'_{\text{deep}}}^{[q+1]}(\mathbf{x}) &= \sigma(\mathbf{W}'^{[q+1]} \mathbf{f}_{\theta'_{\text{deep}}}^{[q]}(\mathbf{x}) + \mathbf{b}'^{[q+1]}) \\ &= \sigma(\mathbf{W}'^{[q+1]} \text{diag}(\boldsymbol{\lambda}) \mathbf{W}'^{[q]} \mathbf{f}_{\theta_{\text{shal}}}^{[q]}(\mathbf{x}) \\ &\quad + \mathbf{W}'^{[q+1]} \text{diag}(\boldsymbol{\lambda}) \mathbf{b}'^{[q]} + \mathbf{W}'^{[q+1]} \boldsymbol{\mu} + \mathbf{b}'^{[q+1]}) \\ &= \sigma(\mathbf{W}^{[q+1]} \mathbf{f}_{\theta_{\text{shal}}}^{[q]}(\mathbf{x}) + \mathbf{b}^{[q+1]}) \\ &= \mathbf{f}_{\theta_{\text{shal}}}^{[q+1]}(\mathbf{x}). \end{aligned}$$

And by recursion, we have  $\mathbf{f}_{\theta'_{\text{deep}}}^{[l]}(\mathbf{x}) = \mathbf{f}_{\theta_{\text{shal}}}^{[l]}(\mathbf{x})$  for  $l \in [q+1 : L]$ .

(ii) By the continuity of the feature function, we know that for any  $\mathbf{x} \in S_{\mathbf{x}}$  there exists at least a neighborhood of  $\mathbf{x}$  such that the layer linearization condition holds. Thus we have  $\mathbf{g}_{\theta'_{\text{deep}}}^{[\hat{q}]}(\mathbf{x}) = \sigma^{(1)}(\mathbf{W}'^{[\hat{q}]} \mathbf{f}_{\theta'_{\text{deep}}}^{[q]}(\mathbf{x}) + \mathbf{b}'^{[\hat{q}]}) = \boldsymbol{\lambda}$ . And the results for feature gradients  $\mathbf{g}_{\theta'_{\text{deep}}}^{[l]}(\mathbf{x})$ ,  $l \in [L]$  can be recursively calculated in a similar way.

(iii) By the backpropagation and the above facts in (i), we have  $\mathbf{z}_{\theta'_{\text{deep}}}^{[L]}(\mathbf{x}) = \nabla \ell(\mathbf{f}_{\theta'_{\text{deep}}}^{[L]}(\mathbf{x}), \mathbf{y}) = \nabla \ell(\mathbf{f}_{\theta_{\text{shal}}}^{[L]}(\mathbf{x}), \mathbf{y}) = \mathbf{z}_{\theta_{\text{shal}}}^{[L]}(\mathbf{x})$ . So for  $l \in [q+1 : L]$ , it is clear that  $\mathbf{z}_{\theta'_{\text{deep}}}^{[l]}(\mathbf{x}) = \mathbf{z}_{\theta_{\text{shal}}}^{[l]}(\mathbf{x})$  and  $\mathbf{z}_{\theta'_{\text{deep}}}^{[\hat{q}]}(\mathbf{x}) = (\mathbf{W}'^{[q+1]})^\top (\mathbf{z}_{\theta_{\text{shal}}}^{[q+1]}(\mathbf{x}) \circ \mathbf{g}_{\theta_{\text{shal}}}^{[q+1]}(\mathbf{x}))$ .

Use the result in (ii), for  $l = q$ ,

$$\begin{aligned} \mathbf{z}_{\theta'_{\text{deep}}}^{[q]}(\mathbf{x}) &= (\mathbf{W}'^{[\hat{q}]})^\top (\mathbf{z}_{\theta'_{\text{deep}}}^{[\hat{q}]}(\mathbf{x}) \circ \mathbf{g}_{\theta'_{\text{deep}}}^{[\hat{q}]}(\mathbf{x})) \\ &= (\mathbf{W}'^{[\hat{q}]})^\top (\mathbf{z}_{\theta'_{\text{deep}}}^{[\hat{q}]}(\mathbf{x}) \circ \boldsymbol{\lambda}). \end{aligned}$$

Since  $\mathbf{f}_{\theta'_{\text{deep}}}^{[l]}(\mathbf{x}) = \mathbf{f}_{\theta_{\text{shal}}}^{[l]}(\mathbf{x})$  and  $\mathbf{g}_{\theta'_{\text{deep}}}^{[l]}(\mathbf{x}) = \mathbf{g}_{\theta_{\text{shal}}}^{[l]}(\mathbf{x})$  for  $l \in [L]$ , we have  $\mathbf{z}_{\theta'_{\text{deep}}}^{[l]}(\mathbf{x}) = \mathbf{z}_{\theta_{\text{shal}}}^{[l]}(\mathbf{x})$  for  $l \in [q-1]$ .  $\square$

**Proposition 4 (network properties preserving).** *Given any  $\text{NN}(\{m_l\}_{l=0}^L)$  and data  $S$ , for any one-layer lifting  $\mathcal{T}_S$  and any network parameter  $\theta_{\text{shal}}$  of NN, the following network properties are preserved for any  $\theta'_{\text{deep}} \in \mathcal{T}_S(\theta_{\text{shal}})$ :*

(i) *outputs are preserved:*  $\mathbf{f}_{\theta'_{\text{deep}}}(\mathbf{x}) = \mathbf{f}_{\theta_{\text{shal}}}(\mathbf{x})$  for  $\mathbf{x} \in S_{\mathbf{x}}$ ;

(ii) *empirical risk is preserved:*  $R_S(\theta'_{\text{deep}}) = R_S(\theta_{\text{shal}})$ ;

(iii) *the network representations are preserved for all layers:*  $\text{span}\{\{(\mathbf{f}_{\theta'_{\text{deep}}}^{[\hat{q}]}(\mathbf{X}))_j\}_{j \in [m'_q]} \cup \{\mathbf{1}\}\} = \text{span}\{\{(\mathbf{f}_{\theta_{\text{shal}}}^{[q]}(\mathbf{X}))_j\}_{j \in [m_q]} \cup \{\mathbf{1}\}\}$ , and for the other index  $l \in [L]$ ,  $\text{span}\{\{(\mathbf{f}_{\theta'_{\text{deep}}}^{[l]}(\mathbf{X}))_j\}_{j \in [m'_l]} \cup \{\mathbf{1}\}\} = \text{span}\{\{(\mathbf{f}_{\theta_{\text{shal}}}^{[l]}(\mathbf{X}))_j\}_{j \in [m_l]} \cup \{\mathbf{1}\}\}$ , where  $\mathbf{f}_{\theta}^{[l]}(\mathbf{X}) = [\mathbf{f}_{\theta}^{[l]}(\mathbf{x}_1), \mathbf{f}_{\theta}^{[l]}(\mathbf{x}_2), \dots, \mathbf{f}_{\theta}^{[l]}(\mathbf{x}_n)]^\top \in \mathbb{R}^{n \times m'_q}$  and  $\mathbf{1} \in \mathbb{R}^n$  is the all-ones vector.

*Proof.* The properties (i) and (ii) are direct consequences of the above lemma.

(iii) It is clear that for  $l \in [L]$

$$\begin{aligned} &\text{span}\{\{(\mathbf{f}_{\theta'_{\text{deep}}}^{[\hat{q}]}(\mathbf{X}))_j\}_{j \in [m'_q]} \cup \{\mathbf{1}\}\} \\ &= \text{span}\{\{(\mathbf{f}_{\theta_{\text{shal}}}^{[q]}(\mathbf{X}))_j\}_{j \in [m_q]} \cup \{\mathbf{1}\}\}. \end{aligned}$$

Since for any  $\mathbf{x} \in S_{\mathbf{x}}$ ,

$$\mathbf{f}_{\theta'_{\text{deep}}}^{[\hat{q}]}(\mathbf{x}) = \boldsymbol{\lambda} \circ (\mathbf{W}'^{[\hat{q}]} \mathbf{f}_{\theta_{\text{shal}}}^{[q]}(\mathbf{x}) + \mathbf{b}'^{[\hat{q}]}) + \boldsymbol{\mu},$$

we have

$$\begin{aligned} &\text{span}\{\{(\mathbf{f}_{\theta'_{\text{deep}}}^{[\hat{q}]}(\mathbf{X}))_j\}_{j \in [m'_q]} \cup \{\mathbf{1}\}\} \\ &= \text{span}\{\{(\mathbf{f}_{\theta_{\text{shal}}}^{[q]}(\mathbf{X}))_j\}_{j \in [m_q]} \cup \{\mathbf{1}\}\}. \end{aligned}$$

Thus we finish the proof.  $\square$

**Proposition 5 (criticality preserving).** *Given any  $\text{NN}(\{m_l\}_{l=0}^L)$  and data  $S$ , for any one-layer lifting  $\mathcal{T}_S$ , if  $\theta_{\text{shal}}$  of NN satisfies  $\nabla_{\theta} R_S(\theta_{\text{shal}}) = \mathbf{0}$ , then  $\nabla_{\theta'} R_S(\theta'_{\text{deep}}) = \mathbf{0}$  for any  $\theta'_{\text{deep}} \in \mathcal{T}_S(\theta_{\text{shal}})$ .*

*Proof.* Gradient of loss with respect to network parameters of each layer can be computed from  $\mathbf{F}$ ,  $\mathbf{G}$ , and  $\mathbf{Z}$  as follows

$$\begin{aligned} \nabla_{\mathbf{W}^{[l]}} R_S(\boldsymbol{\theta}) &= \nabla_{\mathbf{W}^{[l]}} \mathbb{E}_S \ell(\mathbf{f}_{\boldsymbol{\theta}}(\mathbf{x}), \mathbf{y}) \\ &= \mathbb{E}_S ((\mathbf{z}_{\boldsymbol{\theta}}^{[l]}(\mathbf{x}) \circ \mathbf{g}_{\boldsymbol{\theta}}^{[l]}(\mathbf{x})) (\mathbf{f}_{\boldsymbol{\theta}}^{[l-1]}(\mathbf{x}))^\top), \\ \nabla_{\mathbf{b}^{[l]}} R_S(\boldsymbol{\theta}) &= \nabla_{\mathbf{b}^{[l]}} \mathbb{E}_S \ell(\mathbf{f}_{\boldsymbol{\theta}}(\mathbf{x}), \mathbf{y}) = \mathbb{E}_S (\mathbf{z}_{\boldsymbol{\theta}}^{[l]}(\mathbf{x}) \circ \mathbf{g}_{\boldsymbol{\theta}}^{[l]}(\mathbf{x})). \end{aligned}$$

Then we have for  $l \neq q, \hat{q}, q+1$ ,

$$\begin{aligned} \nabla_{\mathbf{W}^{[l]}} R_S(\theta'_{\text{deep}}) &= \nabla_{\mathbf{W}^{[l]}} R_S(\theta'_{\text{deep}}) = \nabla_{\mathbf{W}^{[l]}} R_S(\theta_{\text{shal}}) = \mathbf{0} \\ &\text{and} \end{aligned}$$

$$\nabla_{\mathbf{b}^{[l]}} R_S(\theta'_{\text{deep}}) = \nabla_{\mathbf{b}^{[l]}} R_S(\theta'_{\text{deep}}) = \nabla_{\mathbf{b}^{[l]}} R_S(\theta_{\text{shal}}) = \mathbf{0}.$$

Also, for  $l = q+1$ ,

$$\begin{aligned} \nabla_{\mathbf{W}^{[q+1]}} R_S(\theta'_{\text{deep}}) &= \mathbb{E}_S \left( \left( \mathbf{z}_{\theta'_{\text{deep}}}^{[q+1]}(\mathbf{x}) \circ \mathbf{g}_{\theta'_{\text{deep}}}^{[q+1]}(\mathbf{x}) \right) \left( \mathbf{f}_{\theta'_{\text{deep}}}^{[\hat{q}]}(\mathbf{x}) \right)^\top \right) \\ &= \mathbb{E}_S \left( \left( \mathbf{z}_{\theta_{\text{shal}}}^{[q+1]}(\mathbf{x}) \circ \mathbf{g}_{\theta_{\text{shal}}}^{[q+1]}(\mathbf{x}) \right) \left[ \sigma \left( \mathbf{W}'^{[\hat{q}]} \mathbf{f}_{\theta_{\text{shal}}}^{[q]}(\mathbf{x}) + \mathbf{b}'^{[\hat{q}]} \right) \right]^\top \right) \\ &= \mathbb{E}_S \left( \left( \mathbf{z}_{\theta_{\text{shal}}}^{[q+1]}(\mathbf{x}) \circ \mathbf{g}_{\theta_{\text{shal}}}^{[q+1]}(\mathbf{x}) \right) \left( \boldsymbol{\lambda} \circ (\mathbf{W}'^{[\hat{q}]} \mathbf{f}_{\theta_{\text{shal}}}^{[q]}(\mathbf{x}) + \mathbf{b}'^{[\hat{q}]}) + \boldsymbol{\mu} \right)^\top \right) \\ &= \mathbb{E}_S \left( \left( \mathbf{z}_{\theta_{\text{shal}}}^{[q+1]}(\mathbf{x}) \circ \mathbf{g}_{\theta_{\text{shal}}}^{[q+1]}(\mathbf{x}) \right) \left( \text{diag}(\boldsymbol{\lambda}) (\mathbf{W}'^{[\hat{q}]} \mathbf{f}_{\theta_{\text{shal}}}^{[q]}(\mathbf{x}) + \mathbf{b}'^{[\hat{q}]}) + \boldsymbol{\mu} \right)^\top \right) \\ &= \mathbb{E}_S \left( \left( \mathbf{z}_{\theta_{\text{shal}}}^{[q+1]}(\mathbf{x}) \circ \mathbf{g}_{\theta_{\text{shal}}}^{[q+1]}(\mathbf{x}) \right) \left( \mathbf{f}_{\theta_{\text{shal}}}^{[q]}(\mathbf{x}) \right)^\top \left( \text{diag}(\boldsymbol{\lambda}) (\mathbf{W}'^{[\hat{q}]})^\top \right) \right) \\ &\quad + \mathbb{E}_S \left( \left( \mathbf{z}_{\theta_{\text{shal}}}^{[q+1]}(\mathbf{x}) \circ \mathbf{g}_{\theta_{\text{shal}}}^{[q+1]}(\mathbf{x}) \right) \left( \text{diag}(\boldsymbol{\lambda}) \mathbf{b}'^{[\hat{q}]} + \boldsymbol{\mu} \right)^\top \right) \\ &= \mathbf{0} \\ &\text{and} \end{aligned}$$

$$\begin{aligned} \nabla_{\mathbf{b}'^{[q+1]}} R_S(\theta'_{\text{deep}}) &= \mathbb{E}_S \left( \mathbf{z}_{\theta'_{\text{deep}}}^{[q+1]}(\mathbf{x}) \circ \mathbf{g}_{\theta'_{\text{deep}}}^{[q+1]}(\mathbf{x}) \right) \\ &= \mathbb{E}_S \left( \mathbf{z}_{\theta_{\text{shal}}}^{[q+1]}(\mathbf{x}) \circ \mathbf{g}_{\theta_{\text{shal}}}^{[q+1]}(\mathbf{x}) \right) = \mathbf{0}. \end{aligned}$$

For  $l = \hat{q}$ ,

$$\begin{aligned} \nabla_{\mathbf{W}^{[\hat{q}]}} R_S(\theta'_{\text{deep}}) &= \mathbb{E}_S ((\mathbf{z}_{\theta'_{\text{deep}}}^{[\hat{q}]}(\mathbf{x}) \circ \mathbf{g}_{\theta'_{\text{deep}}}^{[\hat{q}]}(\mathbf{x})) (\mathbf{f}_{\theta'_{\text{deep}}}^{[q]}(\mathbf{x}))^\top) \\ &= \mathbb{E}_S ((\text{diag}(\boldsymbol{\lambda}) \mathbf{z}_{\theta'_{\text{deep}}}^{[\hat{q}]}(\mathbf{x})) (\mathbf{f}_{\theta'_{\text{deep}}}^{[q]}(\mathbf{x}))^\top) \\ &= \mathbb{E}_S ((\text{diag}(\boldsymbol{\lambda}) (\mathbf{W}'^{[q+1]})^\top (\mathbf{z}_{\theta'_{\text{deep}}}^{[q+1]}(\mathbf{x}) \circ \mathbf{g}_{\theta'_{\text{deep}}}^{[q+1]}(\mathbf{x}))) (\mathbf{f}_{\theta_{\text{shal}}}^{[q]}(\mathbf{x}))^\top) \\ &= \text{diag}(\boldsymbol{\lambda}) (\mathbf{W}'^{[q+1]})^\top \mathbb{E}_S ((\mathbf{z}_{\theta'_{\text{deep}}}^{[q+1]}(\mathbf{x}) \circ \mathbf{g}_{\theta'_{\text{deep}}}^{[q+1]}(\mathbf{x})) (\mathbf{f}_{\theta_{\text{shal}}}^{[q]}(\mathbf{x}))^\top) \\ &= \mathbf{0} \end{aligned}$$

and

$$\begin{aligned}
\nabla_{\mathbf{b}'^{[\hat{q}]}} R_S(\boldsymbol{\theta}'_{\text{deep}}) &= \mathbb{E}_S \left( \mathbf{z}_{\boldsymbol{\theta}'_{\text{deep}}}^{[\hat{q}]}(\mathbf{x}) \circ \mathbf{g}_{\boldsymbol{\theta}'_{\text{deep}}}^{[\hat{q}]}(\mathbf{x}) \right) \\
&= \text{diag}(\boldsymbol{\lambda})(\mathbf{W}'^{[q+1]})^\top \mathbb{E}_S \left( \mathbf{z}_{\boldsymbol{\theta}'_{\text{deep}}}^{[q+1]}(\mathbf{x}) \circ \mathbf{g}_{\boldsymbol{\theta}'_{\text{deep}}}^{[q+1]}(\mathbf{x}) \right) \\
&= \text{diag}(\boldsymbol{\lambda})(\mathbf{W}'^{[q+1]})^\top \mathbb{E}_S \left( \mathbf{z}_{\boldsymbol{\theta}'_{\text{shal}}}^{[q+1]}(\mathbf{x}) \circ \mathbf{g}_{\boldsymbol{\theta}'_{\text{shal}}}^{[q+1]}(\mathbf{x}) \right) \\
&= \mathbf{0}.
\end{aligned}$$

For  $l = q$ ,

$$\begin{aligned}
\nabla_{\mathbf{W}'^{[q]}} R_S(\boldsymbol{\theta}'_{\text{deep}}) &= \mathbb{E}_S \left( (\mathbf{z}_{\boldsymbol{\theta}'_{\text{deep}}}^{[q]}(\mathbf{x}) \circ \mathbf{g}_{\boldsymbol{\theta}'_{\text{deep}}}^{[q]}(\mathbf{x})) (\mathbf{f}_{\boldsymbol{\theta}'_{\text{deep}}}^{[q-1]}(\mathbf{x}))^\top \right) \\
&= \mathbb{E}_S \left( ((\mathbf{W}'^{[q]})^\top (\mathbf{z}_{\boldsymbol{\theta}'_{\text{deep}}}^{[q]}(\mathbf{x}) \circ \mathbf{g}_{\boldsymbol{\theta}'_{\text{deep}}}^{[q]}(\mathbf{x})) \circ \mathbf{g}_{\boldsymbol{\theta}'_{\text{deep}}}^{[q]}(\mathbf{x})) (\mathbf{f}_{\boldsymbol{\theta}'_{\text{deep}}}^{[q-1]}(\mathbf{x}))^\top \right) \\
&= \text{diag}(\boldsymbol{\lambda})(\mathbf{W}'^{[q]})^\top (\mathbf{W}'^{[q+1]})^\top \mathbb{E}_S \left( ((\mathbf{z}_{\boldsymbol{\theta}'_{\text{deep}}}^{[q+1]}(\mathbf{x}) \circ \mathbf{g}_{\boldsymbol{\theta}'_{\text{deep}}}^{[q+1]}(\mathbf{x})) \right. \\
&\quad \left. \circ \mathbf{g}_{\boldsymbol{\theta}'_{\text{deep}}}^{[q]}(\mathbf{x})) (\mathbf{f}_{\boldsymbol{\theta}'_{\text{deep}}}^{[q-1]}(\mathbf{x}))^\top \right) \\
&= (\mathbf{W}'^{[q+1]})^\top \mathbb{E}_S \left( ((\mathbf{z}_{\boldsymbol{\theta}'_{\text{deep}}}^{[q+1]}(\mathbf{x}) \circ \mathbf{g}_{\boldsymbol{\theta}'_{\text{deep}}}^{[q+1]}(\mathbf{x})) \right. \\
&\quad \left. \circ \mathbf{g}_{\boldsymbol{\theta}'_{\text{deep}}}^{[q]}(\mathbf{x})) (\mathbf{f}_{\boldsymbol{\theta}'_{\text{deep}}}^{[q-1]}(\mathbf{x}))^\top \right) \\
&= (\mathbf{W}'^{[q+1]})^\top \mathbb{E}_S \left( ((\mathbf{z}_{\boldsymbol{\theta}'_{\text{shal}}}^{[q+1]}(\mathbf{x}) \circ \mathbf{g}_{\boldsymbol{\theta}'_{\text{shal}}}^{[q+1]}(\mathbf{x})) \right. \\
&\quad \left. \circ \mathbf{g}_{\boldsymbol{\theta}'_{\text{shal}}}^{[q]}(\mathbf{x})) (\mathbf{f}_{\boldsymbol{\theta}'_{\text{shal}}}^{[q-1]}(\mathbf{x}))^\top \right) \\
&= \mathbb{E}_S \left( (\mathbf{z}_{\boldsymbol{\theta}'_{\text{shal}}}^{[q]}(\mathbf{x}) \circ \mathbf{g}_{\boldsymbol{\theta}'_{\text{shal}}}^{[q]}(\mathbf{x})) (\mathbf{f}_{\boldsymbol{\theta}'_{\text{shal}}}^{[q-1]}(\mathbf{x}))^\top \right) \\
&= \mathbf{0}
\end{aligned}$$

and

$$\begin{aligned}
\nabla_{\mathbf{b}'^{[\hat{q}]}} R_S(\boldsymbol{\theta}'_{\text{deep}}) &= \mathbb{E}_S \left( \mathbf{z}_{\boldsymbol{\theta}'_{\text{deep}}}^{[q]}(\mathbf{x}) \circ \mathbf{g}_{\boldsymbol{\theta}'_{\text{deep}}}^{[q]}(\mathbf{x}) \right) \\
&= \mathbb{E}_S \left( (\mathbf{W}'^{[\hat{q}]} )^\top \left( \mathbf{z}_{\boldsymbol{\theta}'_{\text{deep}}}^{[\hat{q}]}(\mathbf{x}) \circ \mathbf{g}_{\boldsymbol{\theta}'_{\text{deep}}}^{[\hat{q}]}(\mathbf{x}) \right) \circ \mathbf{g}_{\boldsymbol{\theta}'_{\text{deep}}}^{[q]}(\mathbf{x}) \right) \\
&= \text{diag}(\boldsymbol{\lambda})(\mathbf{W}'^{[\hat{q}]})^\top (\mathbf{W}'^{[q+1]})^\top \mathbb{E}_S \left( (\mathbf{z}_{\boldsymbol{\theta}'_{\text{deep}}}^{[q+1]}(\mathbf{x}) \circ \mathbf{g}_{\boldsymbol{\theta}'_{\text{deep}}}^{[q+1]}(\mathbf{x})) \right. \\
&\quad \left. \circ \mathbf{g}_{\boldsymbol{\theta}'_{\text{deep}}}^{[q]}(\mathbf{x}) \right) \\
&= (\mathbf{W}'^{[q+1]})^\top \mathbb{E}_S \left( \left( \mathbf{z}_{\boldsymbol{\theta}'_{\text{deep}}}^{[q+1]}(\mathbf{x}) \circ \mathbf{g}_{\boldsymbol{\theta}'_{\text{deep}}}^{[q+1]}(\mathbf{x}) \right) \circ \mathbf{g}_{\boldsymbol{\theta}'_{\text{deep}}}^{[q]}(\mathbf{x}) \right) \\
&= (\mathbf{W}'^{[q+1]})^\top \mathbb{E}_S \left( \left( \mathbf{z}_{\boldsymbol{\theta}'_{\text{shal}}}^{[q+1]}(\mathbf{x}) \circ \mathbf{g}_{\boldsymbol{\theta}'_{\text{shal}}}^{[q+1]}(\mathbf{x}) \right) \circ \mathbf{g}_{\boldsymbol{\theta}'_{\text{shal}}}^{[q]}(\mathbf{x}) \right) \\
&= \mathbb{E}_S \left( \mathbf{z}_{\boldsymbol{\theta}'_{\text{shal}}}^{[q]}(\mathbf{x}) \circ \mathbf{g}_{\boldsymbol{\theta}'_{\text{shal}}}^{[q]}(\mathbf{x}) \right) \\
&= \mathbf{0}.
\end{aligned}$$

Collecting all the above relations, we obtain that  $\nabla_{\boldsymbol{\theta}'} R_S(\boldsymbol{\theta}'_{\text{deep}}) = \mathbf{0}$ .  $\square$

**Theorem 2 (embedding principle in depth).** *Given any  $\text{NN}'(\{m_l\}_{l=0}^{L'})$  and data  $S$ , for any  $\boldsymbol{\theta}_c$  of any shallower  $\text{NN}(\{m_l\}_{l=0}^L)$  satisfying  $\nabla_{\boldsymbol{\theta}} R_S(\boldsymbol{\theta}_c) = \mathbf{0}$ , there exists parameter  $\boldsymbol{\theta}'_c$  in the loss landscape of  $\text{NN}'(\{m_l\}_{l=0}^{L'})$  satisfying the following conditions:*

- (i)  $\mathbf{f}_{\boldsymbol{\theta}'_c}(\mathbf{x}) = \mathbf{f}_{\boldsymbol{\theta}_c}(\mathbf{x})$  for  $\mathbf{x} \in S_{\mathbf{x}}$ ;
- (ii)  $\nabla_{\boldsymbol{\theta}'} R_S(\boldsymbol{\theta}'_c) = \mathbf{0}$ .

*Proof.* We prove this theorem by construction using the critical liftings. Let  $J = L - L'$ . The  $J$ -layer lifting  $\mathcal{T}_S$

is the  $J$ -step composition of one-layer liftings, say  $\mathcal{T}_S = \mathcal{T}_S^J \cdots \mathcal{T}_S^2 \mathcal{T}_S^1$ . From Lemma 1, we know one-layer lifting always exists, which leads to the existence of  $J$ -layer lifting  $\mathcal{T}_S$ , i.e.,  $\mathcal{T}_S(\boldsymbol{\theta}_c) \neq \emptyset$  for any  $\boldsymbol{\theta}_c$ . Now we prove by induction that  $J$ -layer lifting  $\mathcal{T}_S$  satisfies the properties of output preserving and criticality preserving.

For  $J = 1$ , Propositions 1 and 2 shows the one-layer lifting satisfies the properties of output preserving and criticality preserving.

Assume that the  $(J - 1)$ -layer lifting satisfies the properties of output preserving and criticality preserving, we want to show that so does the  $J$ -layer lifting.

From the induction hypothesis, we only need to show that if given two critical liftings  $\mathcal{T}_S^1$  and  $\mathcal{T}_S^2$ , then  $\mathcal{T}_S^2 \mathcal{T}_S^1$  also satisfies the properties of output preserving and criticality preserving.

- (i)  $\mathcal{T}_S^2 \mathcal{T}_S^1$  satisfies the property of output preserving:

Since  $\mathcal{T}_S^1$  satisfies the property of output preserving, then for any  $\mathbf{x} \in S_{\mathbf{x}}$  and  $\boldsymbol{\theta}' \in \mathcal{T}_S^1(\boldsymbol{\theta})$ ,  $\mathbf{f}_{\boldsymbol{\theta}'}(\mathbf{x}) = \mathbf{f}_{\boldsymbol{\theta}}(\mathbf{x})$ . Similarly for  $\mathcal{T}_S^2$ , we have for any  $\boldsymbol{\theta}'' \in \mathcal{T}_S^2 \mathcal{T}_S^1(\boldsymbol{\theta})$ ,  $\mathbf{f}_{\boldsymbol{\theta}''}(\mathbf{x}) = \mathbf{f}_{\boldsymbol{\theta}'}(\mathbf{x})$ , hence  $\mathbf{f}_{\boldsymbol{\theta}''}(\mathbf{x}) = \mathbf{f}_{\boldsymbol{\theta}}(\mathbf{x})$ , for any  $\mathbf{x} \in S_{\mathbf{x}}$ .

- (ii)  $\mathcal{T}_2 \mathcal{T}_1$  satisfies the property of criticality preserving:

Since  $\boldsymbol{\theta}$  is a critical point of  $R_S(\boldsymbol{\theta})$ , for any  $\boldsymbol{\theta}' \in \mathcal{T}_S^1(\boldsymbol{\theta})$ ,  $\boldsymbol{\theta}'$  is also a critical point of  $R_S(\boldsymbol{\theta})$ . Similarly, for any  $\boldsymbol{\theta}'' \in \mathcal{T}_S^2(\boldsymbol{\theta}')$ ,  $\boldsymbol{\theta}''$  is also a critical point of  $R_S(\boldsymbol{\theta})$ , hence for any  $\boldsymbol{\theta}'' \in \mathcal{T}_S^2 \mathcal{T}_S^1(\boldsymbol{\theta})$ ,  $\boldsymbol{\theta}''$  is also a critical point of  $R_S(\boldsymbol{\theta})$ .

Therefore, for any  $\boldsymbol{\theta}'_c \in \mathcal{T}_S(\boldsymbol{\theta}_c)$ , conditions (i) and (ii) are satisfied.  $\square$

**Proposition 6 (data dependency of lifting).** *Given any  $\text{NN}(\{m_l\}_{l=0}^L)$  and data  $S$ , for any critical lifting  $\mathcal{T}_S$  and any parameter  $\boldsymbol{\theta}_{\text{shal}}$  of  $\text{NN}$ , if data  $S' \subseteq S$ , then  $\mathcal{T}_S(\boldsymbol{\theta}_{\text{shal}}) \subseteq \mathcal{T}_{S'}(\boldsymbol{\theta}_{\text{shal}})$ .*

*Proof.* We first assume  $\mathcal{T}_S$  is a one-layer lifting. If  $S' \subseteq S$ , i.e., dataset  $S'$  is a subset of dataset  $S$ , then we have  $S'_{\mathbf{x}} \subseteq S_{\mathbf{x}}$ . For any  $\boldsymbol{\theta}'_{\text{deep}} \in \mathcal{T}_S(\boldsymbol{\theta}_{\text{shal}})$ , local-in-layer condition is satisfied regardless of input data. Regarding the data-dependent layer linearization condition, we have that for any  $j \in [m_{\hat{q}}]$ , there exists an affine subdomain  $(a_j, b_j)$  associated with  $\lambda_j, \mu_j$  such that the  $j$ -th component  $(\mathbf{W}'^{[\hat{q}]} \mathbf{f}_{\boldsymbol{\theta}'_{\text{deep}}}^{[\hat{q}]}(\mathbf{x}) + \mathbf{b}'^{[\hat{q}]})_j \in (a_j, b_j)$  for any  $\mathbf{x} \in S_{\mathbf{x}}$ , where  $\mathbf{W}'^{[\hat{q}]}$  and  $\mathbf{b}'^{[\hat{q}]}$  are weight and bias of  $\boldsymbol{\theta}'_{\text{deep}}$  at layer  $\hat{q}$ . Since  $S'_{\mathbf{x}} \subseteq S_{\mathbf{x}}$ , for any  $\mathbf{x} \in S'_{\mathbf{x}}$ , naturally,  $(\mathbf{W}'^{[\hat{q}]} \mathbf{f}_{\boldsymbol{\theta}'_{\text{deep}}}^{[\hat{q}]}(\mathbf{x}) + \mathbf{b}'^{[\hat{q}]})_j \in (a_j, b_j)$ , i.e.,  $\boldsymbol{\theta}'_{\text{deep}}$  satisfies layer linearization condition for  $S'$  with the same  $\boldsymbol{\lambda}$  and  $\boldsymbol{\mu}$  as for  $S$ . Therefore,  $\boldsymbol{\theta}'_{\text{deep}}$  also satisfies the output preserving condition for  $S'$ . Then, we have  $\boldsymbol{\theta}'_{\text{deep}} \in \mathcal{T}_{S'}(\boldsymbol{\theta}_{\text{shal}})$ , which leads to  $\mathcal{T}_S(\boldsymbol{\theta}_{\text{shal}}) \subseteq \mathcal{T}_{S'}(\boldsymbol{\theta}_{\text{shal}})$ .

If  $\mathcal{T}_S$  is a composition of critical liftings that satisfy this corollary, say  $\mathcal{T}_S = \mathcal{T}_S^2 \mathcal{T}_S^1$ . We have for any  $\boldsymbol{\theta}'_{\text{deep}} \in \mathcal{T}_S(\boldsymbol{\theta}_{\text{shal}})$ , there exists  $\boldsymbol{\theta}_{\text{mid}} \in \mathcal{T}_S^1(\boldsymbol{\theta}_{\text{shal}})$  such that  $\boldsymbol{\theta}'_{\text{deep}} \in \mathcal{T}_S^2(\boldsymbol{\theta}_{\text{mid}})$ . Then  $\boldsymbol{\theta}'_{\text{deep}} \in \mathcal{T}_{S'}^2(\boldsymbol{\theta}_{\text{mid}})$  and  $\boldsymbol{\theta}_{\text{mid}} \in \mathcal{T}_{S'}^1(\boldsymbol{\theta}_{\text{shal}})$ .

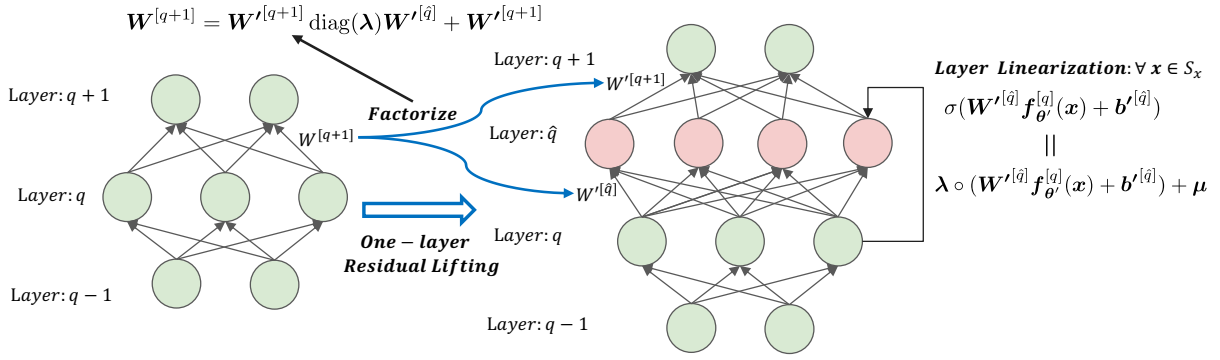


Figure A1: Illustration of one-layer residual lifting. The pink layer is inserted into the left network to get the right network. The input parameters  $\mathbf{W}'^{[\hat{q}]}$  and output parameters  $\mathbf{W}'^{[q+1]}$  of the inserted layer are obtained by factorizing the input parameters  $\mathbf{W}^{[q+1]}$  of  $(q+1)$ -th layer in the left network to satisfy layer linearization and output preserving conditions.

Therefore,  $\theta_{\text{deep}} \in \mathcal{T}_S^2, \mathcal{T}_{S'}^1(\theta_{\text{shal}}) = \mathcal{T}_{S'}(\theta_{\text{shal}})$ , which leads to  $\mathcal{T}_S(\theta_{\text{shal}}) \subseteq \mathcal{T}_{S'}(\theta_{\text{shal}})$ .  $\square$

**Proposition 7.** Given any  $\text{NN}'(\{m'_l\}_{l=0}^{L'})$  and data  $S$ , for any  $\theta_c$  of any shallower  $\text{NN}(\{m_l\}_{l=0}^L)$ , there exists parameter  $\theta'_c$  in the loss landscape of  $\text{NN}'(\{m'_l\}_{l=0}^{L'})$  satisfying the following condition: for any  $\mathbf{x}_i \in S_{\mathbf{x}}$ , there exists a neighbourhood  $N(\mathbf{x}_i)$  of  $\mathbf{x}_i$  such that  $\mathbf{f}_{\theta'_c}(\mathbf{x}) = \mathbf{f}_{\theta_c}(\mathbf{x})$  for any  $\mathbf{x} \in N(\mathbf{x}_i)$ ;

*Proof.* We only prove this result for one-layer lifting and similar to Theorem 1, the result of multi-layer lifting can be easily obtained by induction. Let  $\mathcal{T}_S$  be any one-layer lifting and  $\theta'_c \in \mathcal{T}_S(\theta_c)$ . By the definition of one-layer lifting, layer linearization condition is satisfied, i.e., for any  $j \in [m_{\hat{q}}]$ , there exists an affine subdomain  $(a_j, b_j)$  associated with  $\lambda_j, \mu_j$  such that the  $j$ -th component  $(\mathbf{W}'^{[\hat{q}]} \mathbf{f}_{\theta'_c}^{[\hat{q}]}(\mathbf{x}_i) + \mathbf{b}'^{[\hat{q}]})_j \in (a_j, b_j)$  for any  $\mathbf{x}_i \in S_{\mathbf{x}}$ . Let  $\mathbf{g}(\mathbf{x}) = \mathbf{W}'^{[\hat{q}]} \mathbf{f}_{\theta'_c}^{[\hat{q}]}(\mathbf{x}) + \mathbf{b}'^{[\hat{q}]}$ , and

$$\varepsilon = \min \{ \mathbf{g}(\mathbf{x}_i)_j - a_j, b_j - \mathbf{g}(\mathbf{x}_i)_j \}.$$

By the continuity of the function  $\mathbf{g}(\mathbf{x})$ , there exists a  $\delta$  neighborhood  $N_\delta(\mathbf{x}_i)$  such that  $|\mathbf{g}(\mathbf{x}_i)_j - \mathbf{g}(\mathbf{x})_j| < \varepsilon$  for any  $\mathbf{x} \in N_\delta(\mathbf{x}_i)$ , which implies that  $\mathbf{g}(\mathbf{x})_j \in (a_j, b_j)$ . Therefore, the layer linearization condition indeed holds not only for each training input but also at least a neighbourhood of each training input.

Similar to Lemma 2, by recursive we can get the NN output function is actually preserved over a broader area of input space including at least a neighbourhood of each training input. Hence if the training dataset is sufficiently large and representative, then our lifting operator effectively preserves the generalization performance.  $\square$

We give the rigorous definition of one-layer residual lifting, which is very similar to one-layer lifting. The only difference is that there is one more item in the output preserving condition due to the skip connection (see Fig. A1 for illustration.)

**Definition 5 (one-layer residual lifting).** Given training data  $S$ , an NN  $(\{m_l\}_{l=0}^L)$  and a one-layer deeper  $\text{NN}'(\{m'_l\}, l \in \{0, 1, 2, \dots, q, \hat{q}, q+1, \dots, L\})$ , suppose  $m'_1 = m_1, \dots, m'_q = m_q, m'_{q+1} = m_{q+1}, \dots, m'_L = m_L$ . The one-layer lifting  $\mathcal{T}_S$  maps any parameter  $\theta = (\mathbf{W}^{[1]}, \mathbf{b}^{[1]}, \dots, \mathbf{W}^{[L]}, \mathbf{b}^{[L]})$  of NN to a manifold  $\mathcal{M}(\mathcal{M} := \mathcal{T}_S(\theta))$  of  $\text{NN}'$ 's parameter space, where  $\mathcal{M}$  is a collection of all  $\theta'$  satisfying the following three conditions:

(i) local-in-layer condition: weights of each layer in  $\text{NN}'$  are inherited from NN except for layer  $\hat{q}$  and  $q+1$ , i.e.,

$$\begin{cases} \theta'_l = \theta_l, & \text{for } l \in [q] \cup [q+2 : L], \\ \theta'_{|\hat{q}} = (\mathbf{W}'^{[\hat{q}]}, \mathbf{b}'^{[\hat{q}]}) \in \mathbb{R}^{m'_{\hat{q}} \times m'_{\hat{q}-1}} \times \mathbb{R}^{m'_{\hat{q}}}, \\ \theta'_{|q+1} = (\mathbf{W}'^{[q+1]}, \mathbf{b}'^{[q+1]}) \in \mathbb{R}^{m'_{q+1} \times m'_{\hat{q}}} \times \mathbb{R}^{m'_{q+1}}, \end{cases}$$

(ii) layer linearization condition: for any  $j \in [m_{\hat{q}}]$ , there exists an affine subdomain  $(a_j, b_j)$  of  $\sigma$  associated with  $\lambda_j, \mu_j$  such that the  $j$ -th component  $(\mathbf{W}'^{[\hat{q}]} \mathbf{f}_{\theta'}^{[\hat{q}]}(\mathbf{x}) + \mathbf{b}'^{[\hat{q}]})_j \in (a_j, b_j)$  for any  $\mathbf{x} \in S_{\mathbf{x}}$ .

(iii) output preserving condition:

$$\begin{cases} \mathbf{W}'^{[q+1]} \text{diag}(\lambda) \mathbf{W}'^{[\hat{q}]} + \mathbf{W}'^{[q+1]} = \mathbf{W}^{[q+1]}, \\ \mathbf{W}'^{[q+1]} \text{diag}(\lambda) \mathbf{b}'^{[\hat{q}]} + \mathbf{W}'^{[q+1]} \mu + \mathbf{b}'^{[q+1]} = \mathbf{b}^{[q+1]}. \end{cases}$$

where  $\lambda = [\lambda_1, \lambda_2, \dots, \lambda_{m_{\hat{q}}}]^\top \in \mathbb{R}^{m'_{\hat{q}}}, \mu = [\mu_1, \mu_2, \dots, \mu_{m_{\hat{q}}}]^\top \in \mathbb{R}^{m'_{\hat{q}}}$ .

## Appendix B: Supplementary Experiments

Here we present the supplementary experiments mentioned in the main text as a supplement to our argument.

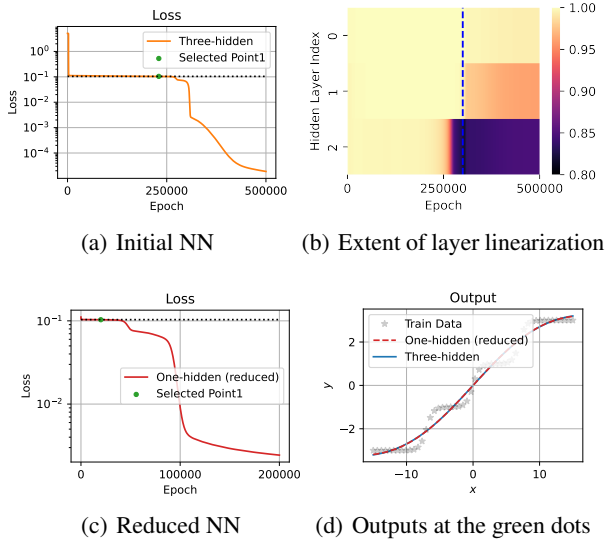


Figure B1: Merging the effectively linear layers of three-hidden-layer NN yields a critical point of the single-hidden-layer NN. (a) Training loss trajectory of the three-hidden-layer NN. The green dot is selected for merging. (b) The extent of layer linearization for different hidden layers during the training process of the three-hidden-layer NN. (c) Training loss trajectory of the reduced single-hidden-layer NN. The black dotted line indicates the same loss value as the black dotted line in (a). The green dot is selected as a representative for comparison. (d) Outputs of the initial and reduced NNs at the training step of green dots.

## Appendix C: Details of Experiments

For the experiment of Iris dataset (Fig. 1 and 4(b)), we use ReLU as the activation function and the mean square error (MSE) as the loss function. We use full-batch gradient descent with learning rate 0.001 to train NNs for 100000 epochs. The width is 50 for each hidden layer. The initial distribution of all parameters follows a normal distribution with a mean of 0 and a variance of 0.07. Remark that, the phenomenon in Fig. 1 are similar for different activation functions.

For the 1-D experiments in Figs. 3, 5, 6, B1, and B2, we use tanh as the activation function and MSE as the loss function. We use full-batch gradient descent with learning rate 0.01 to train NNs with width 50 for each hidden layer. The initial distribution of all parameters follows a normal distribution with a mean of 0 and a variance of 0.01.

For the experiment of MNIST classification (Fig. 7), we use tanh as the activation function and the cross-entropy as the loss function. We use stochastic gradient descent with batch size 1000 and learning rate 0.001 to train NNs for 100 epochs. The width is 50 for each hidden layer. The initial distribution of all parameters follows a normal distribution with a mean of 0 and a variance of 0.05.

For the 1-D experiments in Figs. B3, we use ReLU as the activation function and MSE as the loss function. We

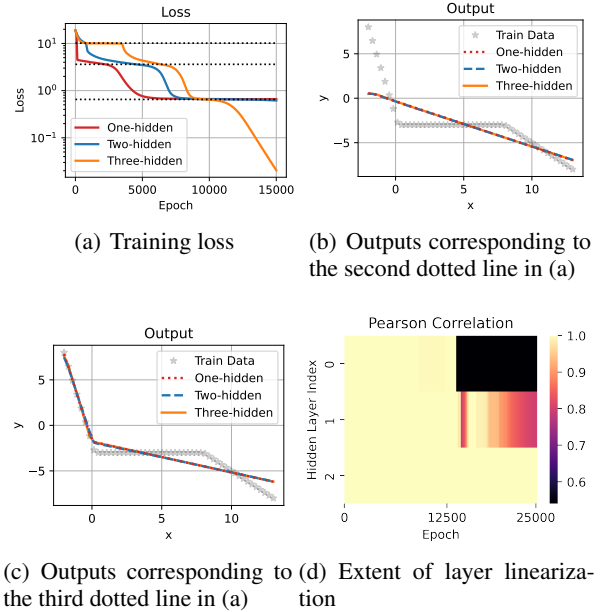


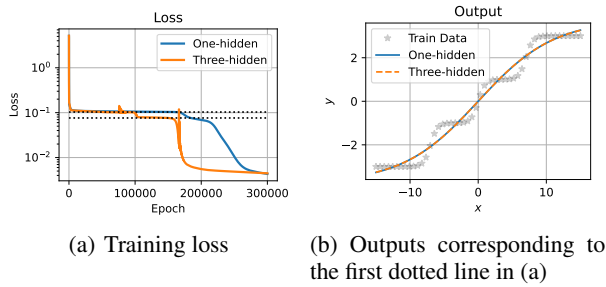
Figure B2: Layer linearization occurs during the stagnation of three-hidden-layer ReLU neural networks. (a) The training loss trajectory for ReLU NN of different depths with 50 neurons in each hidden layer on training data in (b). (b, c) The output functions of NNs with different depths at the same loss values indicated by (b) the second horizontal dotted line or (c) the third horizontal dotted line in (a). (d) The extent of layer linearization for all hidden layers during the training process of three-hidden-layer NN.

use full-batch gradient descent with learning rate 0.001 to train NNs with width 50 for each hidden layer. The initial distribution of all parameters follows a normal distribution with a mean of 0 and a variance of 0.005.

For the experiments in Fig. 4 and B4, we first roughly estimate the possible interval of critical points by observing where the loss decays very slowly and then take the point with the smallest derivative of the parameters (use  $L_1$  norm) as an empirical critical point. The  $L_1$  norm of the derivative of loss function at the empirical critical point is approximately  $10^{-4}$ , which are reasonably small.

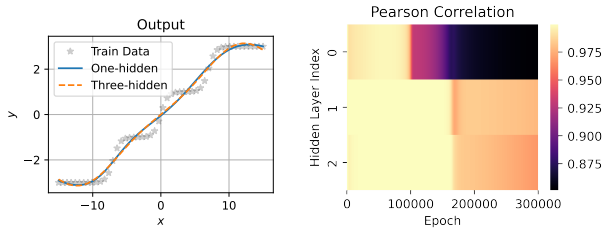
For activation functions with strong nonlinearity near zero (e.g. ReLU), we first removes those “zero-neurons” whose input and output weights are reasonably small to avoid their interference to the measure of layer linearization.

Remark that, although Figs. 1 and 3 are case studies each based on a random trial, similar phenomenon can be easily observed as long as the initialization variance is properly small, i.e., far from the linear/kernel/NTK regime.



(a) Training loss

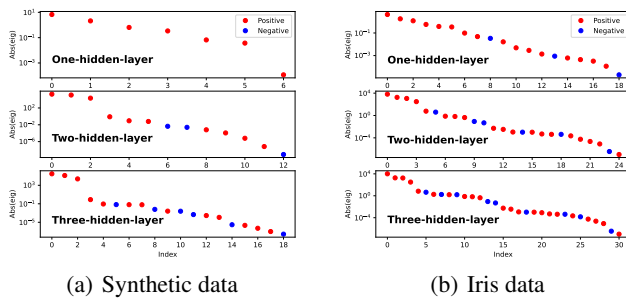
(b) Outputs corresponding to the first dotted line in (a)



(c) Outputs corresponding to the second dotted line in (a)

(d) Extent of layer linearization

Figure B3: Layer linearization occurs during the stagnation of three-hidden-layer residual NN. (a) The training loss for NNs of different depths with 50 neurons in each hidden layer for training data in (b). (b, c) The output functions of NNs with different depths at the same loss values indicated by (b) the first horizontal dotted line or (c) the second horizontal dotted line. (d) The extent of layer linearization for all hidden layers during the training process of three-hidden-layer residual NN.



(a) Synthetic data

(b) Iris data

Figure B4: Eigenvalues of Hessian of NNs at the critical points lifted from the tanh NN with 1 hidden layer for learning data of Fig. 3(b) in (a) and for Iris dataset in (b). We do the lifting operation by factorizing one hidden layer into  $k$  hidden layers ( $k = 2, 3$ ), whose input weights are scaled identity and biases are selected to translate the input range into the approximately linear segment  $[-0.01, 0.01]$  of tanh.